Thermodynamic Modeling and Mechanical Design of a Liquid Nitrogen Vaporization and Pressure Building Device

Brian J. Leege

A thesis

submitted in partial fulfillment of the

requirements for the degree of

Master of Science in Aeronautics & Astronautics

University of Washington

2017

Reading Committee:

Carl Knowlen, Chair

Owen Williams

Program Authorized to Offer Degree:

Aeronautics & Astronautics

University of Washington

Abstract

Thermodynamic Modeling and Mechanical Design of a Liquid Nitrogen Vaporization and Pressure Building Device

Brian J. Leege

Chair of the Supervisory Committee:
Dr. Carl Knowlen, Research Associate Professor
William E. Boeing Department of Aeronautics & Astronautics

The design of a liquid nitrogen vaporization and pressure building device that has zero product waste while recovering some of its stored energy is of interest for the cost reduction of nitrogen for use in industrial processes. Current devices may waste up to 30% of the gaseous nitrogen product by venting it to atmosphere. Furthermore, no attempt is made to recover the thermal energy available in the coldness of the cryogen. A seven step cycle with changing volumes and ambient heat addition is proposed, eliminating all product waste and providing the means of energy recovery from the nitrogen. This thesis discusses the new thermodynamic cycle and modeling as well as the mechanical design and testing of a prototype device. The prototype was able to achieve liquid nitrogen vaporization and pressurization up to 1000 psi, while full cycle validation is ongoing with promising initial results.

TABLE OF CONTENTS

LIST OF FIGURES

LIST OF TABLES

ACKNOWLEDGEMENTS

First, I would like to thank my advisor, Professor Carl Knowlen, for giving me the opportunity to work on this project. He provided significant insight and aid in my development of the new thermodynamic cycle and my modeling effort. The numerous long meetings in his office were invaluable and helped me to think more critically about my own design and modeling decisions. Also, his instruction on the operation and safety of cryogenic systems was critical for the success of this project.

I would also like to thank my colleague, Randon Kimura, for his help and support working on this project together. He provided invaluable support in the manufacturing and assembly of many of the components of this system. Also, he provided significant moral support while working some long hours in lab and when things didn't quite work out as expected.

Thank you to the numerous undergraduate volunteers who worked in the lab and helped with a lot of the system assembly, machining, and testing. You were all a great help and I am deeply grateful for the time you volunteered, as I know how little free time you all have available as engineering students.

This project was sponsored by Air Liquide. Thank you for providing us with an interesting and challenging project and for providing valuable feedback and suggestions throughout the project.

Finally, I would like to thank my family for supporting me throughout my education and showing interest in my work, despite maybe not quite understanding it.

Chapter 1. INTRODUCTION

Nitrogen is an inert gas that is used extensively throughout several industries for manufacturing and production processes. Its uses range from blanketing gases for metals production or machining processes, to purging systems for pharmaceutical or chemical production processes [1]. To improve the economics of transporting nitrogen to the end user, nitrogen is shipped as a cryogenic liquid (LN_2) due to its gaseous to liquid volume ratio of about 700:1. While on site at an industrial facility, the LN_2 is stored in large vacuum-insulated dewars. Since many production processes require gaseous nitrogen near room temperature, a device is needed to vaporize and heat up the nitrogen. In addition, many users need the nitrogen pressurized up to a few hundred psi greater than the pressure of the supply dewar.

Currently, these vaporization and pressure building devices operate on a cycle that requires venting the nitrogen product to atmosphere, resulting in up to 30% product loss. This research focuses on designing a new cycle and mechanical device that can produce the pressurized gaseous nitrogen with zero product loss. In addition, this research seeks to take advantage of the large energy potential of the LN_2 and recover as much energy from it as possible. To this end, we attempt to utilize additional ambient heating to over-pressurize the nitrogen and expand it through a generator to produce power. These two improvements could significantly reduce product waste and the overall cost of nitrogen for the end users. The resulting device is essentially a liquid nitrogen powered engine. The concepts studied in this thesis build off the previous work on liquid nitrogen powered automobiles at the University of Washington [2][3][4].

The pressure builder designs discussed in this thesis make use of a novel ambient heat exchange system to achieve the required room temperature nitrogen output. Existing heat exchanger systems cannot warm the nitrogen up to ambient temperatures without significant icing on their surfaces, requiring multiple heat exchanger systems that must be alternatively cycled for deicing between uses. The new "frost-free" ambient vaporizer heat exchanger system builds off of concepts developed at the University of Washington and its study of liquid nitrogen automobiles and is discussed in the thesis by Kimura [5][6].

The goal of this work is twofold: develop and model a new thermodynamic cycle for the vaporization and pressure building of LN_2, and to design, fabricate, and test a prototype device in lab. The new device must be able to pressurize LN_2 from a 200 psi supply dewar up to a at least 1000 psi and discharge gaseous nitrogen at a nominal mass flow rate of 10 g/s, without venting any nitrogen to atmosphere. While a turbine generator is considered in the design and modeling of the proposed thermodynamic cycles, the mechanical design and integration of a turbine into the prototype is not explored in this work. The thermodynamic cycle development and modeling is discussed in Chapter 2 while the mechanical design of the prototype is discussed in Chapter 3. Testing and validation, as well as the relevant conclusions and future work are discussed in Chapter 4 and Chapter 5, respectively.

Chapter 2. THERMODYNAMIC CYCLE DESIGN AND MODELING

This chapter begins by discussing the generalized thermodynamic cycle used by pressure building devices in industry today. Two alternative cycles are then proposed. First, a cycle utilizing cryogenic refrigeration is discussed, followed by its model development and some basic results. The modeling results elucidated an issue with the cryogenic refrigeration design, leading to the second cycle design utilizing changing pressure builder volumes. Then, model development for the second cycle design is discussed, followed by more detailed results of the whole cycle as well as each individual process.

2.1 EXISTING THERMODYNAMIC CYCLE

The generalized thermodynamic cycle for existing pressure builders consists of four repeating steps: (1) mass fill, (2) pressure building, (3) discharge, and (4) pressure reduction. Step (1) is a straightforward process where the pressure builder volume is filled with LN_2 from the supply dewar. This process was not altered in any of our designs or models.

Step (2) is the process of vaporization and pressure building, usually achieved by ambient heat addition. This process utilizes the large temperature difference between the cryogenic fluid and the ambient surroundings to provide heat to vaporize the liquid cryogen, rapidly building pressure. Once vaporized, the cryogenic gas is further heated to generate an even higher pressure and to maintain a constant, high pressure during discharge in step (3).

The pressurized gas is discharged from the pressure builder in step (3). This is achieved, as stated above, by utilizing ambient heat addition to maintain a constant pressure during discharge. This process proceeds until the pressure builder reaches a state at which the reduced temperature

difference with the surroundings is unable to sustain a high enough rate of heat input to achieve the desired output flow rate.

Finally, in step (4), the high-pressure gas that remains in the pressure builder after discharge must have its pressure reduced below the dewar supply pressure. This pressure reduction of the remainder gas allows the process to close and be repeated. Current industrial machines achieve this step by simply venting the remainder gas to atmosphere, wasting the product. This step is the primary focus of this study as it is desirable to achieve this pressure reduction without wasting any product.

2.2 Cryogenic Refrigeration as a Method for Pressure Reduction

The first method of pressure reduction considered was cryogenic refrigeration. This method would utilize a closed refrigeration loop that would cool the remainder gas down, so that the pressure drops below that of the supply dewar. This results in a saturated mixture of liquid and gaseous nitrogen in the pressure builder volume, thus the "cryogenic refrigeration" moniker. This process would achieve pressure reduction to allow for mass fill, while eliminating all product loss. Due to the mechanical design challenges involved with cryogenic refrigeration, the mechanical design of the refrigeration cycle was ignored while a simple thermodynamic model was considered to determine the feasibility of its implementation into the overall cycle.

2.2.1 *Cryogenic Refrigeration Cycle Design and Modeling*

The proposed cryogenic refrigeration cycle has four steps and the working fluid is assumed to be nitrogen. At state (1), low pressure, saturated vapor is pumped up to high pressure, achieving state (2). The high pressure and relatively warm nitrogen then rejects heat at constant pressure into the pressure builder volume, reaching state (3). Note that this heat rejection step requires an

extra step be added to the overall thermodynamic cycle and will be addressed in the next section. It is assumed that heat is rejected until the working fluid in the refrigeration cycle becomes a saturated liquid. The working fluid is then expanded through a throttle valve, providing further cooling, ending at state (4). Finally, the cooled, low pressure nitrogen absorbs heat from the pressure builder volume, cooling the remainder gas in the pressure builder and returning to state (1).

A model was developed using the cycle and the assumed states described above. A low pressure of 65 psi was chosen, corresponding to a saturation temperature of 93 K, which is a temperature low enough to allow sufficient heat transfer to cool the remainder gas, lowering the pressure below the expected supply dewar pressure of 200 psi. The pump compression ratio and efficiency were assumed to be 4 and 80%, respectively. The cycle is solved using thermodynamic property lookup tables for each state and the process for solving refrigeration cycles as described in the text by Çengel and Boles [7].

There are two important results from this model. First, the two temperatures of the heat exchange process are needed to determine the physical viability of the refrigeration in the overall thermodynamic cycle. The heat absorption occurs at T_1 = 93 K, as prescribed above. Heat rejection occurs at T_3 = 114 K, the saturation temperature at the high pressure of 260 psi. This means that in order for the heat rejection step to be physically possible, the nitrogen in the pressure builder volume must remain below 114 K while it absorbs the rejected heat. The second important result is the ratio of heat rejection to heat absorption, Q_r, obtained by the following equation.

$$Q_r = \frac{h_2 - h_3}{h_1 - h_4} \tag{2.1}$$

In the above equation, h_1, h_2, h_3, and h_4 are the enthalpies at each state. Q_r is 1.4 for the proposed cycle and is used in the overall cycle model to determine the amount of heat that needs to be added back into the nitrogen in the pressure builder, given the amount of heat rejected in the pressure reduction step. This is critical to ensuring that the refrigeration process remains a closed cycle. The full thermodynamic cycle with the added steps for refrigeration will be discussed in the next section, followed by a discussion of the thermodynamic modeling.

2.2.2 *Modification of Thermodynamic Cycle with Refrigeration Cycle Included*

The existing four-step thermodynamic cycle must be modified to accommodate for the refrigeration cycle. As discussed in the previous section, an additional step must be added to account for the heat rejection portion of the refrigeration cycle. Also, because the heat rejection and heat absorption steps of the refrigeration cycle occur simultaneously between two pressure builder volumes at different states, multiple pressure builders are required. Due to the timing of the additional steps, there must be at least three connected pressure builders for the cycle to work. Thus, for this pressure building concept, three pressure builders are assumed to always be in use. Now that multiple pressure builders are being considered, it makes sense to add a venting step from a pressure builder at higher pressure to a pressure builder at lower pressure as a pre-cooling, pressure reduction step. This both reduces the pressure and the amount of mass in the pressure builder, reducing the load on the refrigeration cycle. Reducing the refrigeration load will prove critical to the viability of this cycle, as will be discussed later.

The modified cycle now consists of seven steps that must be appropriately sequenced between three separate pressure builders. The full list of cycle steps is shown in Table 2.1.

Table 2.1. Thermodynamic Cycle Processes with Cryogenic Refrigeration

Process #	Process Description
1	Mass fill from supply dewar
2	Refrigeration – Heat addition
3	Vent fill from higher pressure volume
4	Pressure building by ambient heat addition
5	Discharge by constant pressure heat addition
6	Vent remainder of gas to lower pressure volume
7	Refrigeration – Heat rejection for pressure reduction

Processes (1), (4), and (5) are unchanged from the existing cycle design. Processes (2) and (7) are both steps of the refrigeration cycle and must be carried out simultaneously with the opposite step in another pressure builder. Processes (3) and (6) are the same pressure builder-to-pressure builder venting process where direction of the process is switched. The cycle sequence for three pressure builders is shown in Table 2.2.

Table 2.2. Thermodynamic Cycle Timeline with Cryogenic Refrigeration and Three Pressure Builders

Process #			Description
PB1	PB2	PB3	
1	-	4/5	Add LN_2 to PB1, Build pressure and discharge PB3
2	7	-	Refrigeration cycle between PB1 and PB2 (Remove heat from PB2 and add heat to PB1)
3	-	6	Vent from PB3 to PB1
4/5	1	-	Add LN_2 to PB2, Build pressure and discharge PB1
-	2	7	Refrigeration cycle between PB2 and PB3 (Remove heat from PB3 and add heat to PB2)
6	3	-	Vent from PB1 to PB2
-	4/5	1	Add LN_2 to PB3, Build pressure and discharge PB2
7	-	2	Refrigeration cycle between PB3 and PB1 (Remove heat from PB1 and add heat to PB3)
-	6	3	Vent from PB2 to PB3

Note that the highlighted rows represent a single physical process that occurs between two pressure builders. Table 2.2 also shows that at least three pressure builders are needed to complete the cycle without venting any nitrogen to atmosphere.

2.3 Development of Thermodynamic Cycle Model with Cryogenic Refrigeration

A model for the thermodynamic cycle with cryogenic refrigeration was developed using the first law of thermodynamics [7]. Each process in the cycle was modeled individually, maintaining the conservation of energy throughout. The flowchart for the full cycle model is shown in Figure 2.1 below. As shown in Figure 2.1, the need for iteration comes from the pressure builder-to-pressure builder venting model, which requires knowledge of a later state in order to carry out the calculations. The model and associated assumptions for each individual process is discussed in the sections below, following the order shown in the flowchart.

The modeling was done using MATLAB software in conjunction with REFPROP. REFPROP is a NIST developed software and thermodynamic property database, used in this case for nitrogen property lookups [8].

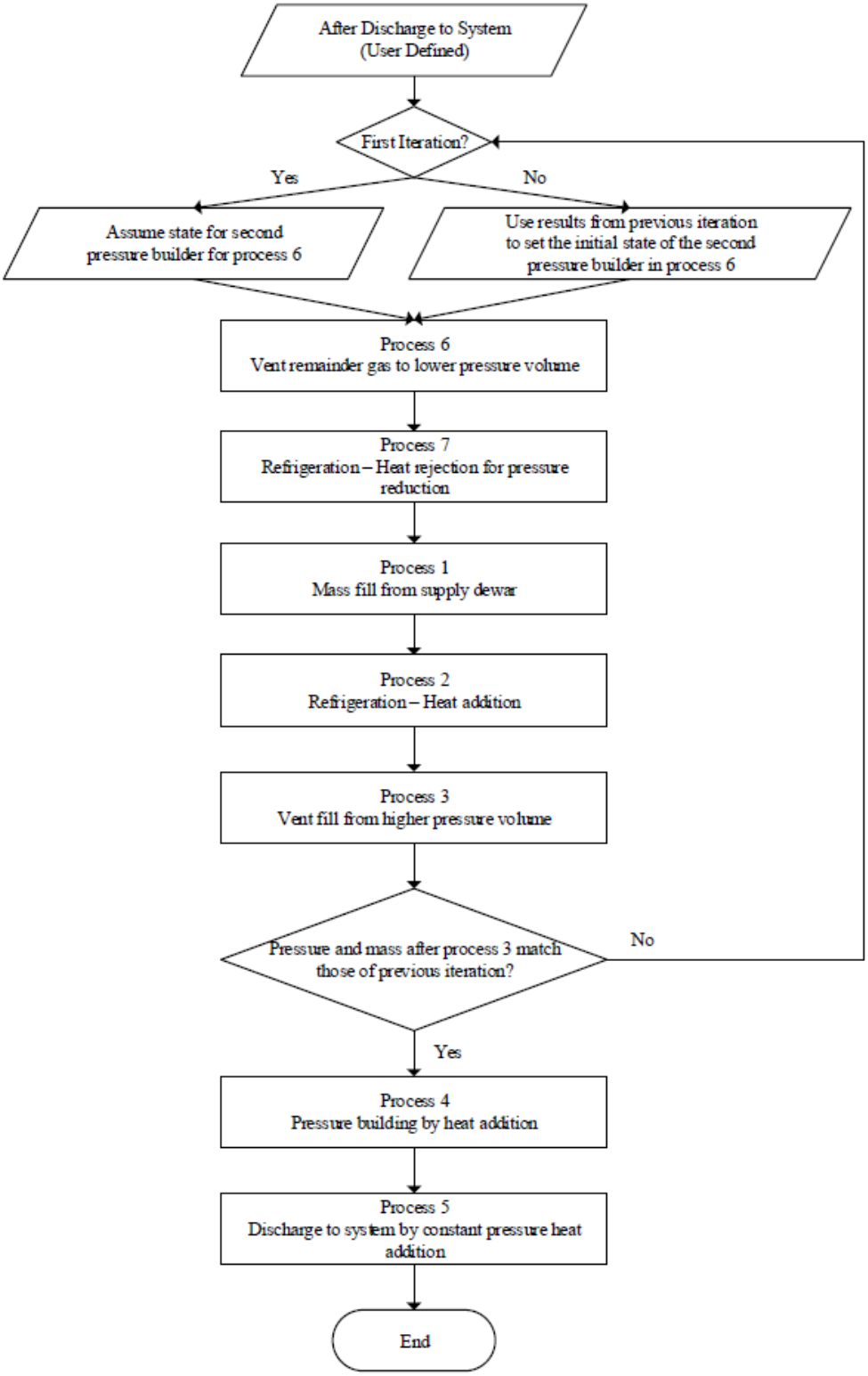

Figure 2.1. Flowchart for the Thermodynamic Cycle Model with Cryogenic Refrigeration.

2.3.1 *Pressure Builder-to-Pressure Builder Vent (Process 6)*

The pressure builder-to-pressure builder venting model simulates the venting from the first pressure builder at high pressure into a second pressure builder at lower pressure. For simplicity, the process is assumed to be adiabatic, although, given a known heat input, this model could be modified to include a heat leak. The first law can be written as

$$E - dE = E' \tag{2.2}$$

where E is the initial energy, dE is the change in energy, and E' is the final energy of the volume after some small time. Since the states in both pressure builders change as the mass is transferred, small mass steps, dm, must be taken to simulate the process, accounting for the new states after each step. A mass step of 0.1 g was used to achieve convergence for this model, as well as all subsequent models that utilize mass steps. Thus, Eq. (2.2) for the first pressure builder (PB1) can be written as

$$m_1 u_1 - dm h_1 = (m_1 - dm) u_1' \tag{2.3}$$

where m_1 is the initial mass in PB1, u_1 is the initial internal energy in PB1, h_1 is the initial enthalpy in PB1, and u_1' is the new internal energy in PB1. Solving Eq. (2.3) for u_1' yields

$$u_1' = \frac{m_1 u_1 - dm h_1}{m_1 - dm}. \tag{2.4}$$

The new density in PB1, ρ_1', is given by

$$\rho_1' = \frac{m_1 - dm}{V} \tag{2.5}$$

where V is the volume of the pressure builder. Using the new internal energy and density inside PB1 given by Eqs. (2.4) and (2.5), the new thermodynamic state in PB1 can be determined through property lookup tables. This process is repeated for a series of small steps in mass until the total mass transfer is achieved.

The state change in the second pressure builder (PB2) is determined by the mass and energy change in PB1. Assuming an adiabatic process with no external work, the energy change, dE, from PB1 is the change in energy in PB2 and Eq. (2.2) still applies. Rewriting Eq. (2.2) for PB2 yields

$$m_2 u_2 + dmh_1 = (m_2 + dm)u_2' \tag{2.6}$$

where m_2 is the initial mass in PB2, u_2 is the initial internal energy in PB2, h_1 is the initial enthalpy in PB1, and u_2' is the new internal energy in PB2. Solving Eq. (2.6) for u_2' yields

$$u_2' = \frac{m_2 u_2 + dmh_1}{m_2 + dm}. \tag{2.7}$$

The new density in PB2, ρ_2', is given by

$$\rho_1' = \frac{m_1 - dm}{V}. \tag{2.8}$$

The new internal energy and density in PB2, given by Eqs. (2.7) and (2.8), can be used to solve for the new thermodynamic state via property lookup tables. This process is also repeated for each small step in mass.

The above procedures are repeated until the pressures in both pressure builders equalize, indicating a cessation of mass transfer. The initial state in the first pressure builder is set by the user. The initial pressure is set at the discharge pressure of 1000 psi. The volume is chosen by the user, setting the size scale for the model. The initial temperature was chosen to be 190 K, limiting the required heat load for discharge. The choice of this temperature will be further discussed with other results in Section 2.4. The pressure, temperature, and volume chosen above set the initial thermodynamic state in the first pressure builder.

The initial thermodynamic state of the second pressure builder must be converged upon by iteration, as discussed in the section above. The pressure is initially assumed to be the supply

dewar pressure and a reasonable mass, with respect to the chosen size scale of the model, must also be assumed. Results from this model are passed on to the heat rejection model, as shown in Figure 2.1.

2.3.2 *Refrigeration – Heat Rejection (Process 7)*

The heat rejection phase of the pressure building cycle is the step where the remainder gas is reduced to a pressure below that of the supply dewar. Heat is rejected through the refrigeration cycle discussed in Chapter 2.2. The initial state is determined from the output of the previous step (pressure builder-to-pressure builder vent). It is also assumed that there is no heat transfer with the surroundings and no external work. Since there is no mass transfer, the final state can be directly determined by setting the desired low pressure. A low pressure of about 90 psi was chosen to allow for sufficient mass fill during the next step. Given the new low pressure and the mass of nitrogen in the pressure builder, the final state is defined and all other properties can be found. The amount of heat rejected, Q_{rej}, can now be calculated.

$$Q_{rej} = m(u - u') \tag{2.9}$$

The heat rejected is used later, along with the heat ratio from Eq. (2.1), to determine the required amount of heat addition for the second part of the refrigeration cycle. The final state of the heat rejection process is passed on to the mass fill model, as shown in Figure 2.1.

2.3.3 *Mass Fill from Supply Dewar (Process 1)*

The next step in the thermodynamic cycle is the mass refill from the supply dewar. Since this step involves mass transfer, small changes in state must be calculated in sequence, similar to the pressure builder-to-pressure builder vent model. The initial state is taken from the heat rejection model output and it is assumed to be an adiabatic process with no external work.

The mass fill process is modeled like the pressure builder-to-pressure builder vent process, except that it is assumed that the supply is a reservoir, having constant thermodynamic properties. Thus, the energy balance for the pressure builder in Eq. (2.2) can be rewritten as

$$mu + dmh_s = (m + dm)u' \tag{2.10}$$

where m is the mass in the pressure builder, u is the internal energy of the pressure builder, dm is the differential change in mass, h_s is the enthalpy of the supply dewar, and u' is the new internal energy in the pressure builder. Therefore, dmh_s is the energy transferred into the pressure builder at each step and remains constant throughout the process. Solving for u' in Eq. (2.10) gives

$$u' = \frac{mu+dmh_s}{m+dm}. \tag{2.11}$$

The new density in the pressure builder can be written as

$$\rho' = \frac{m+dm}{V}. \tag{2.12}$$

The new thermodynamic state is defined by these two quantities and the rest of the state properties can be obtained. This process is repeated until the pressure builder pressure reaches that of the supply dewar, stopping mass transfer. The final state of this process is then passed on to the heat addition model, as shown in Figure 2.1.

2.3.4 *Refrigeration – Heat Addition (Process 2)*

The heat addition part of the cycle is the process where heat is rejected from the refrigeration cycle and added to the pressure builder, thus closing the refrigeration cycle. Like the heat rejection process, the change in state can be directly calculated from using the total amount of heat addition since there is no mass transfer. It is assumed there is no heat transfer with the surroundings or external work.

The required amount of heat addition is calculated using the total heat rejected and the heat ratio as determined by Eqs. (2.9) and (2.1), respectively. Thus, the required heat addition, Q_{add}, is

$$Q_{add} = Q_{rej}Q_r \, . \tag{2.13}$$

Knowing Q_{add}, (2.2) can be rewritten as

$$mu + Q_{add} = mu' \tag{2.14}$$

where m is the mass in the pressure builder, u is the initial internal energy in the pressure builder, and u' is the final internal energy in the pressure builder. Solving for u' in Eq. (2.14) gives

$$u' = \frac{mu+Q_{add}}{m} \, . \tag{2.15}$$

Since mass is constant, density is constant, and the new thermodynamic state can be obtained using the new internal energy and density.

The final state of this process is the initial state of the second pressure builder in the pressure builder-to-pressure builder vent process discussed in section 2.3.1. To ensure consistency within the overall model, these states must match. Therefore, the four processes discussed above are repeated until the states converge. Acceptable convergence was determined to be when the pressure difference was less than 1 psi and the mass difference was less than 10 grams. In each iteration, the final state calculated from the heat addition model was used for the initial state of the second pressure builder in the pressure builder-to-pressure builder venting model. In most cases, the model converged after less than seven iterations. After convergence is achieved, the remaining steps in the cycle can be modeled.

2.3.5 *Pressure Builder-to-Pressure Builder Vent (Process 3)*

The pressure builder-to-pressure builder vent process is identical to the previously modeled process discussed in section 2.3.1, except in this step the pressure builders are switched. That is, in this step, the pressure builder receives mass from a higher pressure volume. To avoid redundancy and to reduce calculation time, the results from the previously converged model are used by switching the results between pressure builders. The final state of this process is passed on to the pressure building by heat addition model, as shown in Figure 2.1.

2.3.6 *Pressure Building by Heat Addition (Process 4)*

Pressure building by ambient heat addition is the next step in the cycle. During this process, the nitrogen in the pressure builder is heated until it reaches the required discharge pressure of 1000 psi. This process was modeled by taking incremental step increases in pressure up to max pressure in order to track the change in temperature throughout the process. The temperature is important because the heat addition requires a temperature difference with ambient air in order to drive the rise in pressure. A pressure step of about 1.5 psi was used in the numerical solution of this model.

At each pressure step, the density remains constant since there is no change in mass. Given the known pressure and density at each step, the remaining thermodynamic properties can be obtained. The heat addition at each step, dQ, is also calculated using

$$dQ = m(u' - u) \tag{2.16}$$

where m is mass, u' is the final internal energy, and u is the initial internal energy. This heat input can be added up for the entire process to help determine the required heating load for the

process. These steps are repeated until the pressure reaches the required discharge pressure. The results of this model are passed on to the discharge model, as shown in Figure 2.1.

2.3.7 *Discharge to System by Constant Pressure Heat Addition (Process 5)*

The final step in the model is discharge to ambient heat exchange system by heat addition at constant pressure. Since mass leaves the system during this process, an incremental approach must be taken. In this case, since the mass flow rate is the required 10 g/s discharge, small steps in time are used. For model convergence, a time step of 0.1 seconds was used, corresponding to a mass step of 1 gram. The entire discharge occurs at constant pressure. It is also assumed that there is no heat transfer with the surroundings and no external work.

At each step the pressure is constant and the mass change in known, so the new density can be calculated as

$$\rho' = \frac{m-dm}{V} \tag{2.17}$$

where m is the initial mass and dm is the change in mass. Knowing the pressure and density, the rest of the thermodynamic properties can be obtained. To find the heat addition that ensures the constant pressure discharge, the first law of thermodynamics is used and Eq. (2.2) is rewritten as

$$mu + dQ - dmh = (m - dm)u' \tag{2.18}$$

where dQ is the heat added, h is the enthalpy in the pressure builder, and u' is the final internal energy in the pressure builder. Solving Eq. (2.18) for dQ gives

$$dQ = (m - dm)u' + dmh - mu\ . \tag{2.19}$$

The heat addition is tracked in order to determine the net required heat input to drive the discharge process while maintaining desired flow rate and pressure. This procedure is repeated at small time and mass steps until the assumed initial state is reached.

2.4 Results of Thermodynamic Cycle Model with Cryogenic Refrigeration

The individual process models discussed in Section 2.3 were combined into a single, comprehensive model that was used to study the proposed cycle. The model, following the flowchart shown in Figure 2.1, was able to converge on multiple closed, self-consistent solutions for the cycle, representing a wide range of input parameters and cycle design decisions.

First, the results of the discharge model were of primary importance to establish a suitable "initial state" for the cycle. Specifically, the temperature of the initial state, immediately after discharge from the pressure builder, was needed to define the initial state at which the model could begin. The discharge process was modeled for a variety of flow rates and physical size scales to determine a suitable end temperature for discharge. Figure 2.2 below shows the heat power required for one case on a laboratory scale model, discharging 500 g of nitrogen at 10 g/s and 1000 psi. The required heat power spikes initially, reduces to a minimum, then rises linearly with temperature. This trend was seen regardless of the size scale and the mass flow rate.

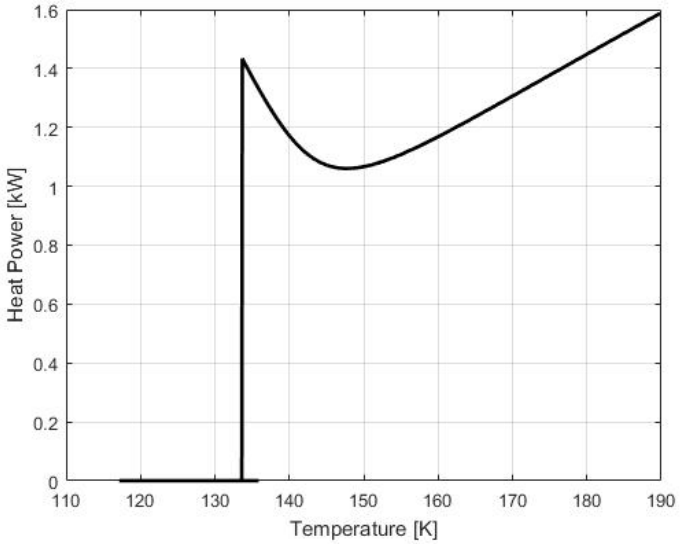

Figure 2.2. Required Heat Power Input During Discharge as a Function of Temperature.

A final temperature of 190 K was chosen to end the discharge process, representing a temperature at which the required heat power reaches just above the initial spike. This temperature is dependent on the discharge pressure. The final temperature was chosen to reduce the maximum required heat load during discharge. If the nitrogen was warmed up further, the temperature difference with ambient would be reduced, making the heat addition significantly more difficult to achieve. Coupled with the trend of increasing heat power requirements, it is practical to stop the process before the required heat load becomes too significant. Additional refinement of an optimal stopping temperature for discharge could be done during experimentation with a full prototype.

The most important result of the model was the observation and subsequent conclusion that the heat addition process, where heat is rejected from the refrigeration cycle, could not be physically achieved for the cycle design. Specifically, the temperature during the heat addition process always rises above the temperature of heat rejection for the refrigeration cycle of about 114 K as stated in Section 2.2.1 above. Figure 2.3 below shows the percent of the required heat added to the pressure builder during process two for a range of high pressures for the refrigeration cycle. The data is for a cycle with 1000 psi discharge, 1.15 kg of discharge, a low pressure in the refrigeration cycle of 65 psi, and a perfectly efficient compressor. At best the best case scenario for a refrigeration cycle high pressure of 400 psi, only about 65 % of the heat could be added to the pressure builder before a temperature equilibrium was reached.

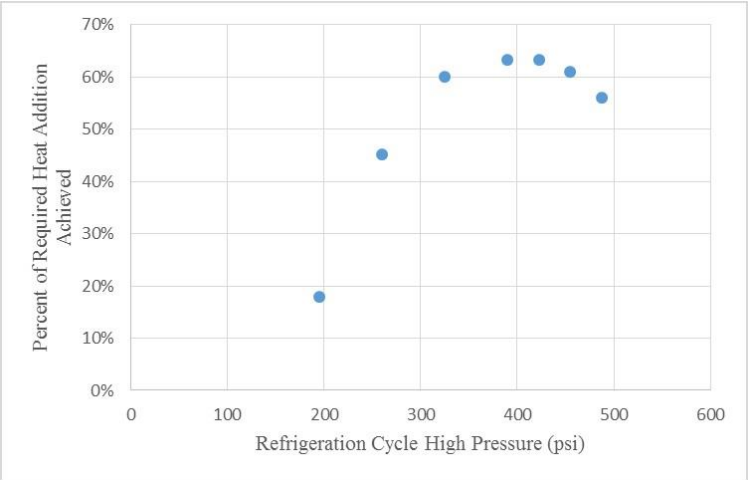

Figure 2.3. Percent of Required Heat Added vs. Refrigeration Cycle High Pressure for the Refrigeration – Heat Addition Process (Process 2).

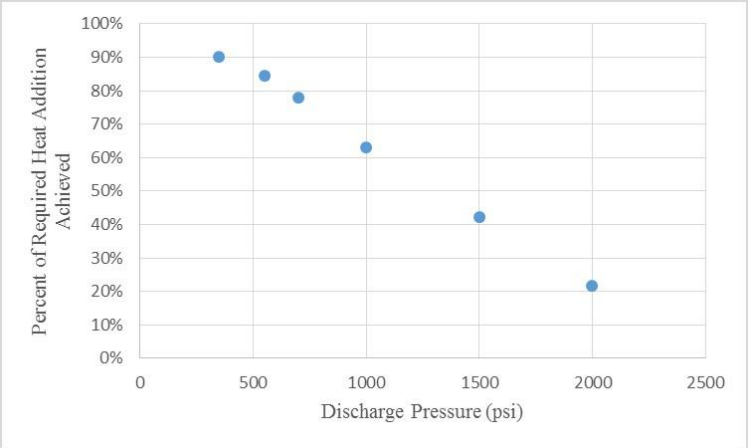

Figure 2.4. Percent of Required Heat Added vs. Discharge Pressure for the Refrigeration – Heat Addition Process (Process 2).

Figure 2.4 above shows the percent of required heat addition for different cycle discharge pressures. The data assumes the same cycle parameters as those in Figure 2.3 and a fixed refrigeration cycle high pressure of about 400 psi, corresponding to the optimum high pressure for maximum heat addition. Figure 2.4 shows that even with minimal pressure building, the heat addition process cannot be fully completed, with a maximum heat added around 90 % under ideal conditions. This shows that even while under ideal conditions, the heat addition step

(Process 2) cannot be completed due to a temperature equilibrium occurring before heat transfer can be completed, meaning the refrigeration cycle as a whole is unfeasible.

While unexpected, the result is reasonable due to the understood difficulty of heat rejection while maintaining cryogenic temperatures. The inherent problem is that a relatively large amount of heat must be added to the pressure builder system while maintaining a low enough temperature to drive the heat transfer. During this process, heat is added at constant density since mass and volume are constant. The constant density heat addition causes a rapid increase in temperature, ultimately eclipsing the refrigerant temperature and stopping the heat transfer. Due to this issue, the cycle as proposed in Sections 2.2 and 2.3 is not a viable option. A proposed solution would be to expand the pressure builder volume during the heat addition process, forcing a constant pressure and temperature heat addition. This approach will be discussed in Sections 2.5 through 2.7 below. Due to the infeasibility of the cryogenic refrigeration process proposed, the rest of the results of this model will be discussed with the modified cycle in Section 2.7.

2.5 Changing Volumes as a Method for Pressure Reduction

The infeasibility of the pressure building cycle with cryogenic refrigeration necessitates the use of changing volumes in order to achieve the proper pressure reduction needed to complete a closed cycle. By considering a change in volume, the refrigeration cycle can be eliminated from the pressure building cycle, avoiding the mechanical design challenges inherent of cryogenic refrigeration and significantly reducing the complexity of the system. Instead, pressure reduction is achieved through the pressure builder-to-pressure builder venting and expansion processes.

The new cycle with changing volumes has seven steps, shown in Table 2.3 below. The heat rejection and heat addition steps from the refrigeration cycle are replaced by mechanical

expansion and compression, respectively. Also, part of the discharge process must now be achieved by mechanical compression, increasing the amount of work input to the system. All other steps of the cycle remain unchanged from the previous cycle design.

Table 2.3. Thermodynamic Cycle Steps with Changing Volume

Process #	Process Description
1	Mass fill from supply dewar
2	Vent fill from higher pressure volume
3	Mechanical compression to max pressure
4	Discharge by mechanical compression to minimum volume
5	Discharge by constant pressure heat addition
6	Vent remainder gas to lower pressure volume
7	Mechanical expansion to max volume

Now that the cycle does not have the two refrigeration steps, and the required synchronization with three or more pressure builders to achieve them, the cycle can be achieved with just two pressure builders, as required by the pressure builder-to-pressure builder venting process. The new thermodynamic cycle sequence, synced between the two pressure builders, is shown in Table 2.4 below.

Table 2.4. Thermodynamic Cycle Timeline with Changing Volumes and Two Pressure Builders

Process #		Description
PB1	PB2	
1	5	Add LN_2 to PB1 and discharge from PB2 by ambient heat addition
2	6	Vent from PB2 to PB1
3	7	Compress PB1 to max pressure and expand PB2 to max volume
4	1	Discharge PB1 by compression and add LN_2 to PB2
5	-	Discharge PB1 by ambient heat addition
6	2	Vent from PB1 to PB2
7	3	Expand PB1 to max volume and compress PB2 to max pressure
-	4	Discharge PB2 by compression

Note that the highlighted rows represent a single physical process that occurs between two pressure builders. While the other processes must still be carried out in order, they do not need to be synched with the other pressure builder.

2.6 Development of Thermodynamic Cycle Model with Changing Volumes

As discussed in the section above, the only new steps in this pressure building cycle are the mechanical compression and expansion steps, replacing the refrigeration steps of the previous cycle. The flowchart for the model is shown in Figure 2.5 below. As can be seen in Figure 2.5, the model still requires iteration to achieve convergence on the initial state of the second pressure builder for the pressure builder-to-pressure builder venting process. For this model, however, the maximum volume must be converged upon in addition to the pressure and mass for the second pressure builder. The model for each process is discussed in the sections below.

2.6.1 *Pressure Builder-to-pressure Builder Vent (Process 6)*

The model for this process is unchanged from that of the previous cycle design discussed in Section 2.3.1. The pressure and temperature for the second pressure builder are assumed as before, according to the supply dewar pressure and discharge pressure, respectively. For this cycle, the volume must also be assumed and is initially guessed as being twice that of the first pressure builder, meaning a volume ratio of two for the system. This proved to be a reasonable estimate for relatively quick convergence.

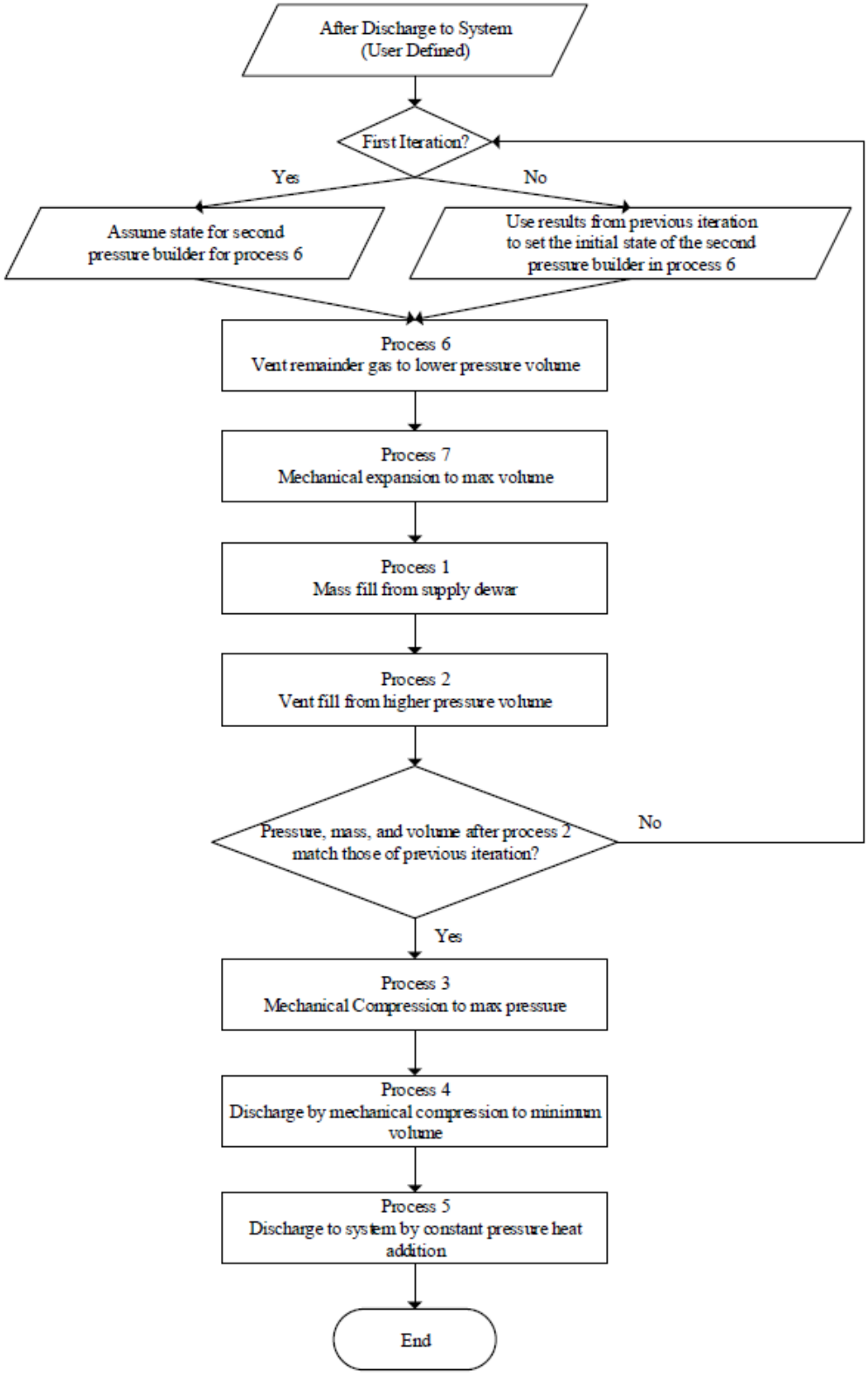

Figure 2.5. Flowchart for the Thermodynamic Cycle Model with Changing Volumes.

2.6.2 *Expansion to Maximum Volume (Process 7)*

The expansion process to max volume acts as the primary pressure reduction step in the proposed cycle. After the pressure is initially reduced in the pressure builder-to-pressure builder venting process, the remaining gas is expanded to reduce the pressure below that of the supply dewar, allowing mass fill. The expansion work done by the fluid, W_{exp}, can be written as

$$W_{exp} = pdV\ , \tag{2.20}$$

where p is pressure and dV is the change in volume. Due to pressure changes throughout the process, small volume steps must be used. Steps of $1\text{x}10^{-6}$ m^3 are used for model convergence.

Assuming an adiabatic expansion, the energy equation from Eq. (2.2) written for each step is

$$mu - pdV = mu' \tag{2.21}$$

where m is mass, u is the initial internal energy, and u' is the final internal energy. Solving Eq. (2.21) for u' yields

$$u' = u - \frac{pdV}{m}\,. \tag{2.22}$$

The new density at each step can be calculated as

$$\rho' = \frac{m}{V+dV} \tag{2.23}$$

where V is the previous volume. Knowing the new internal energy and density at each step, the rest of the thermodynamic state properties can be obtained. This process is repeated at incremental volume changes until the maximum volume is reached. The final pressure should now be below that of the supply dewar, allowing the cryogen mass fill process to occur.

2.6.3 *Mass Fill from Supply Dewar (Process 1)*

This process is unchanged from that of the previous cycle design discussed in Section 2.3.3.

2.6.4 *Pressure Builder-to-pressure Builder Vent (Process 2)*

This is the same process as that discussed in Section 2.6.1 (process 6), except that in this case mass is vented into the pressure builder from a higher pressure volume. As with the previous cycle model, the results of the process 6 model are flipped and used for this process, saving computation time.

2.6.5 *Compression to Maximum Pressure (Process 3)*

The compression step is necessary to return the pressure builder to its minimum volume so that the volume can be expanded again after discharge. In this step, the volume is compressed to some intermediate volume because the nitrogen reaches its maximum pressure before the minimum volume is reached. Because of this, some mass is discharged by compression until the pressure builder returns to the minimum volume, as will be discussed in Section 2.6.6.

The work spent to compress the volume can be written as

$$W_{comp} = pdV\ , \tag{2.24}$$

where p is pressure and dV is the change in volume. Due to the changing pressures throughout the process, the compression must be calculated using incremental changes in volume, using the same volume step as the expansion model to ensure model convergence. Assuming adiabatic compression, the energy equation Eq. (2.2) can be rewritten as

$$mu + pdV = mu' \tag{2.25}$$

where m is mass, u is the initial internal energy, and u' is the final internal energy. Solving for u' yields

$$u' = u + \frac{pdV}{m}\,. \tag{2.26}$$

The new density at each step can be calculated as

$$\rho' = \frac{m}{V - dV} \tag{2.27}$$

where V is the previous volume. The remaining thermodynamic state properties can now be obtained using the new density and internal energy. This procedure is repeated at each volume step until the pressure reaches the maximum cycle pressure, ending at some volume between the minimum and maximum volumes. The work, W_{comp}, is also tracked at each step to determine how much total external work must be added to the system to achieve the desired compression. This will be important in determining the net energy balance for the cycle.

2.6.6 *Discharge to System by Compression (Process 4)*

A portion of the nitrogen must be discharged to the system by compression since the volume does not reach the minimum volume by the time maximum pressure is achieved. This compression discharge is modeled as a two-step, incremental process. Since a desired flow rate must be achieved, the discharge is incremented temporally, just as the heat addition discharge process. This allows for the calculation of the required compression power for discharge. During the first step, mass leaves the system at the prescribed flow rate for the duration of the time step. During the second step, assuming no time change, the volume is compressed back to the original maximum pressure. It is also assumed that there is no heat exchange with the environment. This two-step process approximates the constant pressure discharge during compression.

The first step is modeled using the energy equation from Eq. (2.2) and rewriting it as

$$mu - \dot{m}dth = (m - \dot{m}dt)u_{int} \tag{2.28}$$

where m is mass, $\dot{m}$ is the desired mass flow rate, dt is the incremental time step, h is the enthalpy, and u_{int} is the internal energy of the intermediate step. Solving Eq. (2.28) for u_{int} gives

$$u_{int} = \frac{mu - \dot{m}dth}{m - \dot{m}dt}. \tag{2.29}$$

The intermediate density can be calculated as

$$\rho_{int} = \frac{m - \dot{m}dt}{V} \tag{2.30}$$

where V is the volume before the time step. Using the intermediate internal energy and density from Eqs. (2.29) and (2.30), the remaining intermediate thermodynamic properties can be obtained.

The second step assumes that the compression occurs immediately after the discharge step and takes no time. If we assume that the nitrogen is an ideal gas and undergoes isentropic compression, the new, compressed volume can be obtained from the equation

$$V' = V\left(\frac{p_{int}}{p_{max}}\right)^{\frac{1}{\gamma}} \tag{2.31}$$

where p_{int} is the intermediate pressure, p_{max} is the max system pressure, and γ is the average specific heat ratio [7]. This equation solves for the volume change of compression that would maintain a constant pressure for the amount of mass that was discharged. By using sufficiently small time steps, this model should work as a good approximation of the actual process. Using the new volume, the new density can be calculated as

$$\rho' = \frac{m - \dot{m}dt}{V'}. \tag{2.32}$$

Using the new density and the known pressure of p_{max}, the remaining thermodynamic properties can be determined for the end state. The work input for each time step can then be calculated as

$$W_{discharge} = p_{max}(V - V') \tag{2.33}$$

and the power input would be

$$P_{discharge} = \frac{p_{max}(V-V')}{dt}. \tag{2.34}$$

These will provide a measure of how much energy and power is needed to mechanically compress the volume to achieve the desired discharge rate and help determine the net energy balance for the cycle.

The two-step process described above is repeated at incremental time steps until the minimum volume for the cycle is reached. Once the volume reaches its minimum, discharge by heat addition begins.

2.6.7 *Discharge to System by Constant Pressure Heat Addition (Process 5)*

This process is identical to that of the previous cycle model discussed in Section 2.3.7, except that the initial state occurs immediately after the discharge by compression process ends. The modeling and end state are unchanged from the previous cycle model.

2.6.8 *Turbine Generator for Energy Recovery*

As discussed in Chapter 1, if the nitrogen is pressurized above the final desired pressure, the gas can be expanded through a turbine generator to recover some of the energy input throughout the cycle. In the model results discussed in Section 2.7, there is about 12 times more heat energy added to the system than mechanical energy. Since a large proportion of the energy input is from ambient heat addition, which is essentially "free" energy, it may be possible to achieve a positive net energy balance.

To determine the recoverable energy, a turbine was modeled assuming a conservative efficiency estimate of 80%. The nitrogen is pressurized to a maximum pressure of 1000 psi

while the final use pressure is assumed to be no higher than 725 psi. It is also assumed that the higher pressure discharge will be warmed to ambient temperature at constant pressure through a series of ambient heat exchangers to add as much "free" energy to the flow as possible.

Given the pressure and temperature of the nitrogen gas before the turbine, the initial thermodynamic properties can be obtained. By assuming a full expansion down to the final pressure, taking into account the turbine efficiency, the enthalpy out of the turbine can be calculated as

$$h_{out} = h - \eta * (h - h_s) \tag{2.35}$$

where h is the initial enthalpy of the nitrogen, η is the turbine efficiency, and h_s is the isentropic enthalpy out of the turbine. Thus, the work out of the turbine is

$$W_{turbine} = m(h - h_{out}) \, , \tag{2.36}$$

where m is the total mass that flows through the turbine. Turbine power is

$$P_{turbine} = \dot{m}(h - h_{out}) \, , \tag{2.37}$$

where $\dot{m}$ is the mass flow rate to the system. Eqs. (2.36) and (2.37) will be used in the calculation of the net energy and power balances for the system, discussed in the following section.

2.6.9 *Net Energy Balance of the Thermodynamic Cycle with Changing Volumes*

The net energy and power balances of the cycle are of key importance when considering both the thermodynamic cycle design and the mechanical design of the system. The net energy balance will determine whether the cycle can operate with or without external energy input and be used as a parameter for optimization. The power balance will show whether the power produced by

the turbine is enough to power the mechanical components of the system, determining if an energy storage device or external power input is needed.

The net energy balance for this cycle will only consider the useful energy produced from the cycle and the work put into the system, ignoring the ambient heat addition since it has no cost. It is also assumed that there is negligible energy or power input for circulation fans for the heat addition process. Therefore, the net energy, E_{net}, is

$$E_{net} = W_{turbine} - W_{comp} - W_{discharge} \, . \tag{2.38}$$

That is, the net energy is the turbine work less the compression and discharge work. If E_{net} is positive, the turbine generates enough energy for the cycle, meaning the cycle is self-sustaining. If E_{net} is negative, external energy input would be required to operate the cycle. The net energy per mass discharged will be of primary interest during cycle optimization.

The only power produced in the cycle is the turbine power. The only process that requires a specific amount of power is the compression discharge process since a specific flow rate is required. Therefore, the net power of the cycle, P_{net}, is

$$P_{net} = P_{turbine} - P_{discharge} \, . \tag{2.39}$$

P_{net} is assumed to be the maximum power during discharge, ensuring that P_{net} is the peak net power for the cycle. If P_{net} is positive, then the turbine produces enough power to power the entire cycle, even during peak power consumption. If P_{net} is negative, then the turbine does not produce enough power at peak conditions and an energy storage device must be used to provide the power required during the compression discharge process. Regardless, an energy storage device will be required to power the compression process since no power is produced during that process.

2.7 Results of Thermodynamic Cycle Model with Changing Volumes

The process models discussed in Section 2.6 were combined into a single comprehensive model, following the flowchart in Figure 2.5. The model was able to converge upon a self-consistent solution for the cycle. The results of the model, for a lab scale device, are presented in Table 2.5 below.

Table 2.5. State Property Results from the Thermodynamic Cycle Model with Changing Volumes at Lab Scale

Process #	**Process Description**	**State Properties After Process**			
		Pressure (psi)	**Temperature (K)**	**Mass (kg)**	**Volume (L)**
1	Mass Fill	175	107	0.80	4.0
2	PB to PB Vent Fill	291	116	0.94	4.0
3	Compression to Max Pressure	1000	133	0.94	1.9
4	Discharge by Compression	1000	131	0.91	1.8
5	Discharge by Heat Addition	1000	190	0.26	1.8
6	PB to PB Vent	291	131	0.12	1.8
7	Expansion	97.3	97.9	0.12	4.0

The minimum volume of the cycle was chosen to be 1.8 liters, setting a reasonable size scale for lab testing. The maximum volume of 4 liters was chosen since it was a large enough volume change to achieve the desired pressure reduction during expansion while reducing the required net energy input for the cycle. The important cycle characteristics are shown in Table 2.6 below.

Table 2.6. Important Cycle Characteristics for the Thermodynamic Cycle Model with Changing Volumes at Lab Scale

Maximum Pressure	1000 psi	Mass Discharged	0.69 kg
Supply Pressure	200 psi	E_{net}	7.18 kJ
Minimum Volume	1.8 L	E_{net}/m	10.5 kJ/kg
Maximum Volume	4.0 L	P_{net}	-0.22 kW

As can be seen in Table 2.6, sufficient energy is produced during the cycle but the power produced by the turbine is not enough to provide the peak power for the compression discharge process. Thus, an energy storage device will be necessary to complete the cycle.

The mass fill process is shown in Figure 2.6 below.

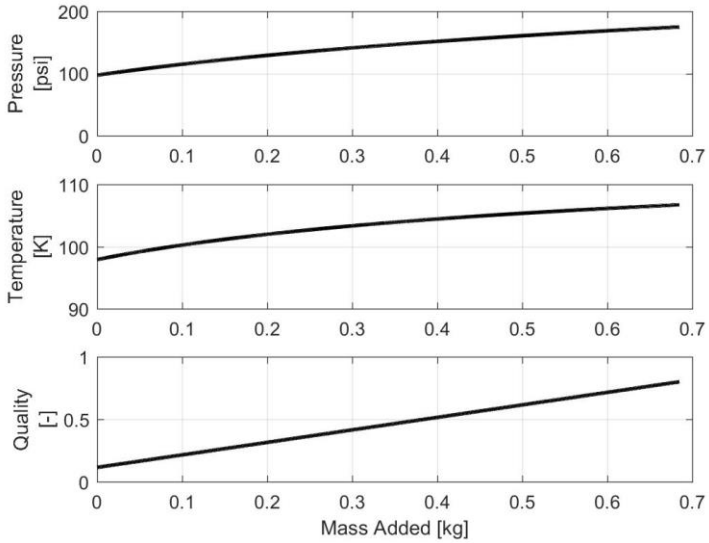

Figure 2.6. Pressure, Temperature, and Quality vs. Mass Added During the Mass Fill Process (Process 1).

It is important to note that during a real mass fill process, the pressure will rise to the supply pressure of 200 psi. In the model, the pressure only rises to 175 psi in order to maintain a mass balance. That is, for the given initial cycle parameters, the model forces a slightly lower end pressure during the mass fill process in order to preserve the mass balance of the whole cycle. It is expected that this discrepancy with expected operation will produce relatively small errors with respect to those from the other model assumptions.

The results of the pressure builder-to-pressure builder venting process are shown in Figure 2.7 and Figure 2.8 below.

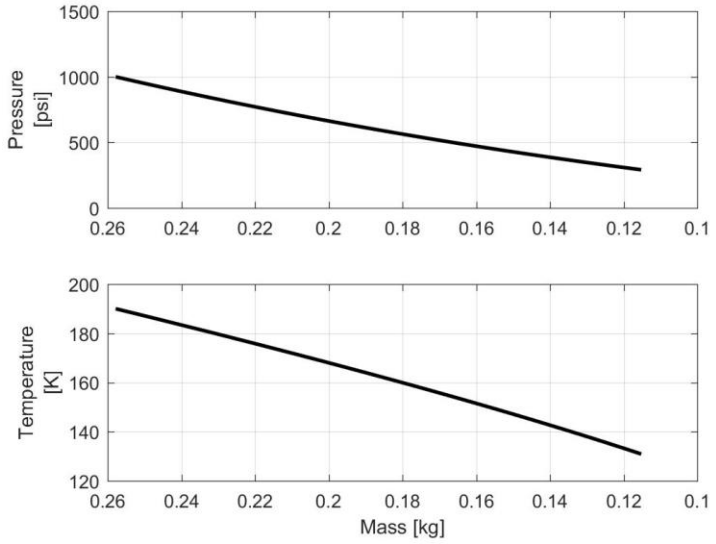

Figure 2.7. Pressure and Temperature vs. Mass During the Pressure Builder-to-Pressure Builder Venting Process (Process 6).

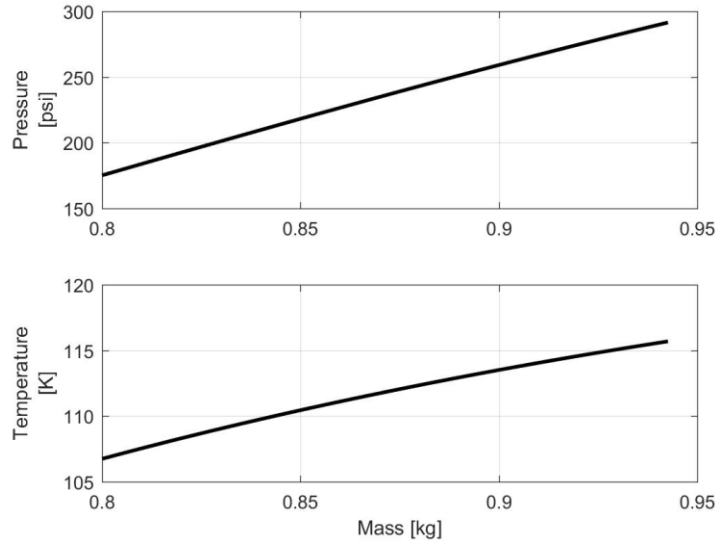

Figure 2.8. Pressure and Temperature vs. Mass During the Pressure Builder-to-Pressure Builder Venting Process (Process 2).

Figure 2.7 shows the high pressure blow-down process while Figure 2.8 shows the low pressure vent-fill process. As can be seen in the above figures, as well as Table 2.5, the pressures equalize as expected while the temperatures do not. The temperatures in each pressure builder are approaching an equilibrium but the final temperature difference is about 15 K. The

temperature discrepancy makes sense because the rate of heat transfer between the fluids in each pressure builder is significantly slower than the rate of mass transfer due to pressure differentials. The pressure drops from 1000 psi to 291 psi and 0.14 kg is transferred during this process. The large pressure drop is ideal for reducing the amount of expansion needed to drop the pressure below the supply pressure.

The results of the expansion process are shown in Figure 2.9 below.

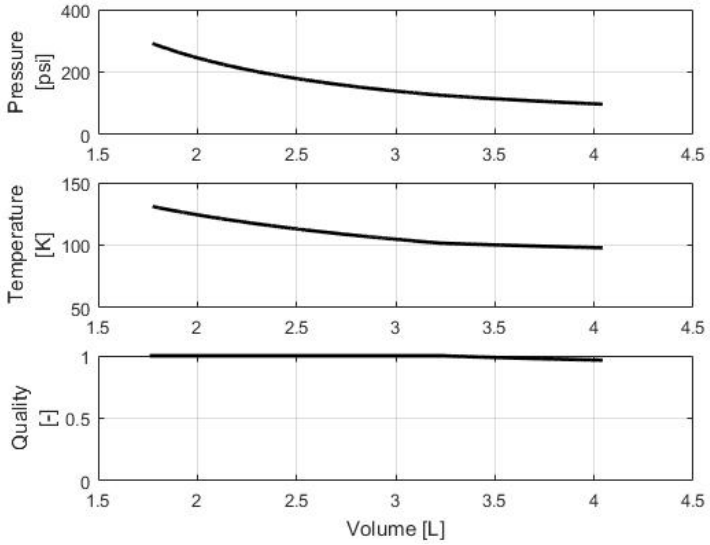

Figure 2.9. Pressure, Temperature, and Quality vs. Volume During the Expansion Process (Process 7).

During this process, pressure is reduced to just under 100 psi, leaving about a 100 psi pressure differential to drive the mass fill process. As discussed above, the volume ratio of about 2.2 for this model was chosen as a reasonable value to achieve the desired pressure reduction while maintaining reasonable energy input requirements during compression.

The results of the compression process are shown in Figure 2.10 below.

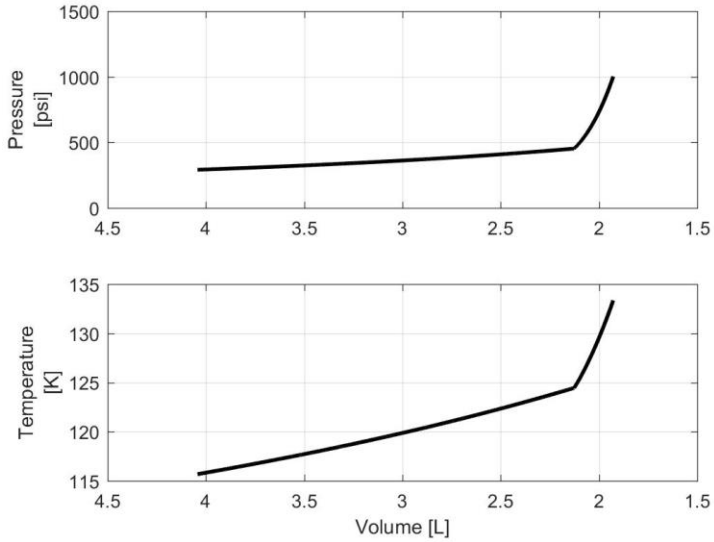

Figure 2.10. Pressure and Temperature vs. Volume During the Compression Process (Process 3).

During compression, the pressure and temperature increase rapidly once the pressure reaches about 492 psi, the critical pressure for nitrogen. The final volume of the compression process is about 1.9 L, meaning that the pressure builder must compress by another 0.1 L during the discharge process to reach the minimum volume for the cycle.

The results of the discharge processes are shown in Figure 2.11 below. Through both processes, 0.69 kg of nitrogen are discharged from the pressure builder. At a controlled flow rate of 10 g/s, the discharge takes about 69 seconds. As can be seen in Figure 2.11, the mechanical power required for compression is less than half the required heat power. Discharge stops when the pressure builder reaches 190 K. At this temperature, the required heat power input reaches just above the initial heat power input, as predicted by the previous model shown in Figure 2.2.

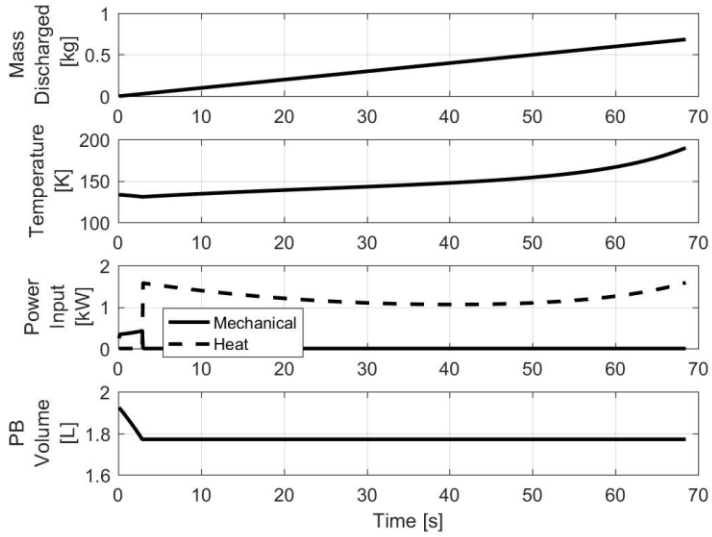

Figure 2.11. Mass Discharged, Temperature, Power Input, and PB Volume vs. Time for the Discharge Processes (Process 4 and 5).

The results of this model show the working steady-state operation of a liquid nitrogen vaporization and pressure building device. Not only is it able to achieve the desired maximum pressure, it is possible to generate more energy than it consumes, meaning that it can operate without external energy input. However, the model makes a series of assumptions that idealizes the processes and a prototype needed to be developed in order to determine the viability of the process and the validity of the model. The model and size scale discussed in this section was used to design a prototype device for use in lab. The mechanical design of the prototype is discussed in Chapter 3.

Chapter 3. MECHANICAL DESIGN OF VAPORIZATION AND PRESSURE BUILDING DEVICE

The mechanical design of the pressure builder prototype utilized the model discussed in the previous sections to aid in the selection of the overall size scale. Minimum and maximum volumes of about 1.4 L and 3.1 L were chosen to preserve the volume ratio of about 2.2. Two different designs were considered for the prototype and both were built. The first design was a single cylinder pressure builder with an internal piston, pneumatically driven by a high-pressure bottle of room temperature nitrogen. A second design was built that utilizes a second, larger diameter cylinder to act as a pressure multiplier to pneumatically drive the piston with a lower pressure source. The first pressure builder design was meant to test the ability to achieve the desired pressurization of 1000 psi. All the single pressure builder processes, expansion, compression, mass fill, and discharge, could also be tested with the first design. The second pressure builder design was meant to provide, in conjunction with the first design, a full two-pressure builder system to test out the remaining processes as well as the cycle in whole. The second pressure builder design would serve as a point of comparison against the first design to explore the feasibility of integrating a lower pressure pneumatic system. The designs will be detailed in Section 3.1 and Section 3.2 below. All mechanical drawings for parts are shown in Appendix A.

3.1 PNEUMATICALLY DRIVEN PRESSURE BUILDER

A cylinder with an outer diameter of 4 inches and a wall thickness of 0.25 inches was chosen for the pressure builder. All material in the design was chosen to be 304 stainless steel for compatibility and strength at cryogenic temperatures. This provided a pressure vessel that could

withstand the 1000 psi maximum pressure at cryogenic temperatures with a factor of safety of about 4 using Barlow's formula for pipe bursting pressure [9]. A cylinder length of 36 inches was chosen to accommodate the chosen volumes while maintaining the flexibility to alter the volumes and test different configurations.

A stainless steel piston was designed to fit the inside of the cylinder, while mitigating the effects of thermal expansion. Utilizing the industrial O-ring standard as a design guide, the cylinder bore, piston size, and piston gland size were determined. Mechanical drawings of both the cylinder and piston are shown in Appendix A. To meet the precision required for the O-ring seals, the cylinder required precision honing.

For the 3.5 inch nominal bore diameter for the tube, an O-ring dash number 338 was required. A significant design challenge was finding a dynamic seal that would hold at cryogenic temperatures. A dynamic cryogenic seal capable of sealing up to 1000 psi is virtually non-existent in industry. One supplier was found that made O-ring seals that are advertised for dynamic cryogenic use. Saint-Gobain has a series of O-ring seals called OmniSeals, which are spring-energized O-ring seals [10]. The seals consist of a sheath that utilizes a spring and the system pressure to help maintain the seal while at cryogenic temperatures. A diagram showing the OmniSeal design and principal of operation is shown in Figure 3.1 below. For this design, an OmniSeal with part number 250-338-A15-05 was used. This utilizes a lubricated glass filled PTFE sheath material which has relatively low friction and high durability, while made for use at cryogenic temperatures. The sheathing material is also self-lubricated, meaning no lubricant is needed in the cylinder that could contaminate the nitrogen product. Two O-rings were used per piston to reduce leak through.

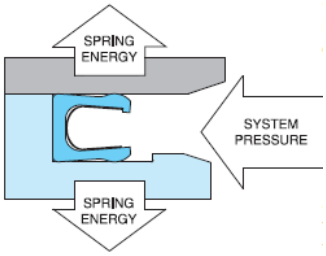

Figure 3.1. OmniSeal Design and Operating Principal [10].

The ends of the cylinder are closed off with flanges. A 304 stainless steel flange was welded to each end of the cylinder and cap flanges were bolted on the ends to seal off the volume. The flanges were 1500# class 2.5-inch pipe size forged flanges with a custom center hole bored out to the 4-inch diameter for the cylinder. The cap flanges have tapped holes in them to allow for the connection of tubing to and from the pressure builder. A full plumbing and instrumentation diagram (P&ID) for the experimental setup can be found in Figure 4.1 and an explanation of the experimental setup will be discussed in Chapter 4. Drawings for the flanges are shown in Appendix A. To seal the cylinder, 2.5-inch pipe size ANSI 150 class metal gaskets with graphite fillers were installed between the flanges. Despite the class ratings and the cryogenic temperatures that the gaskets saw, they maintained a sufficient seal throughout the lifetime of the prototype, including a hydrostatic pressure test up to 3000 psi.

To handle the heat addition phase of the cycle, a coiled copper tube heat exchanger was constructed and installed within the cylinder. A 0.25-inch copper tube was used for bendability and ease of fabrication for the coil. The coiled tube mounts to the flange using Swagelok tube and NPT fittings.

To ensure that the piston stops at the minimum and maximum volumes for the cycle, mechanical stops were added. The stops consisted of 0.75-inch diameter threaded steel rod that is threaded into the flanges. To ensure the proper minimum and maximum volumes, the stops

were cut to 7.37 inches and 13 inches, respectively. The volume of the rods as well as the heat exchanger coils were considered when determining the rod lengths to ensure the model volumes were achieved. With the stop lengths as indicated above and the overall cylinder length of 36 inches, the pressure builder stroke is 14.38 inches. The extra 13 inches of dead volume on the warm side of the cylinder allows for significant flexibility in the actual volumes and volume ratios used in the experiments.

3.2 Pressure Builder with Pneumatically Driven Pressure Multiplier

A pneumatically driven pressure multiplier was designed to drive the compression process while using a lower pressure source since this would be required in the end use product. Specifically, the compression needed to be achieved using a pressure source less than 150 psi, allowing use of standard shop-air supplies. To achieve this, a second piston-cylinder device was designed with an inner diameter of 10 inches, providing a pressure ratio of 8.16. Thus, compression up to 1000 psi in the smaller diameter, cold volume can be achieved with just 123 psi on the larger diameter, warm volume. Once again, dimensions were driven by the industrial standard O-ring design with dash number 448. The cylinder length was kept at 36 inches for compatibility with the smaller diameter cylinder. The large cylinder was made from carbon steel instead of stainless steel since it only experiences ambient temperatures. The mechanical drawings for both the piston and the cylinder can be found in Appendix A.

The pressure multiplier piston was designed to be connected to the smaller piston with a tie rod. The original design was for a 0.75-inch diameter, 28-inch long steel rod threaded into the pressure multiplier piston and freely pushing up against the small piston. An aluminum crosshead was designed to be attached to the free hanging end to eliminate transverse loads on the rod and reduce the possibility of buckling. In effect, this would make both ends fixed, except

for torsional loads which should be minimal, significantly reducing the probability of buckling. Using Euler's buckling equation, a factor of safety of 5 was achieved for the design. However, after initial testing, the tie rod buckled. The buckling most likely occurred due to non-axial loading on the tie rod in conjunction with small vibrations introduced during motion. Thus, a new tie rod was designed with a diameter of 1.5 inches. The rod would be turned down to 0.75 inches at one end to be compatible with the existing pressure multiplier piston. By doubling the diameter of the tie rod, the factor of safety for buckling increased to 80. The drawing for the tie rod can be found in Appendix A.

The pressurized end of the pressure multiplier cylinder is sealed off with a welded carbon steel flange with a cap flange bolted on. On the non-pressurized side, a carbon steel flange was welded on. A matching stainless steel flange was welded onto the non-pressurized end of the stainless steel cylinder. The two flanges are bolted together with spacers that allow air flow in and out of the unpressurized sides of both cylinders. A 150# class metal gasket with graphite filler was used to seal the flange connection. All flanges are 10-inch pipe size 150# class forged flanges. The welded steel flanges have a custom 10.6 inch bore hole while the welded stainless steel flange has a custom 4-inch diameter bore hole. Drawings for all flanges can be found in Appendix A.

A full assembly rendering for a single pressure builder device including labeled features is pictured in Figure 3.2 below. Note that this rendering excludes the crosshead, external piping connections, piston stops, and all mounting and connecting hardware.

The full experimental apparatus, including both pressure builders and all plumbing and instrumentation will be discussed with the full experimental setup in Chapter 4.

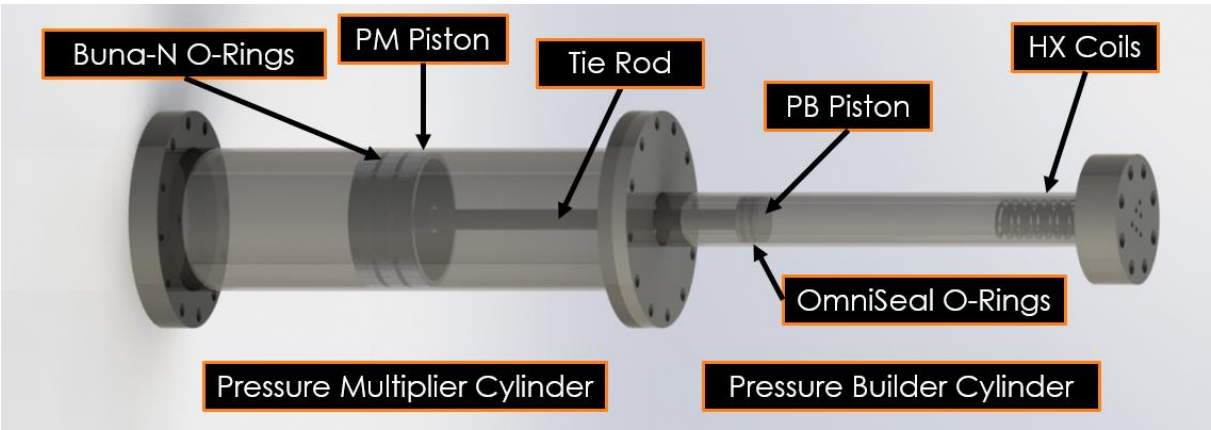

Figure 3.2. Pressure Builder with Pneumatic Pressure Multiplier Assembly.

Chapter 4. TESTING AND VALIDATION

Testing for the prototype began with the pneumatically driven pressure builder design. Initial tests were conducted to determine the effectiveness of the seals and to see if the pressure could be built up to 1000 psi with the system. Later, tests were conducted to determine the validity of a few of the process models. After testing with a single pressure builder was exhausted, the second pressure builder with the pressure multiplier was constructed to test the full cycle. At this time, it was determined that the piston seals were not working effectively enough to conduct appropriate testing of the system. The experimental setup of the prototype system is discussed in the next section, followed by a discussion of each test and their results.

4.1 Experimental Setup

Only the experimental setup of the full, two pressure builder system will be discussed in this section. The setup of the initial, single pressure builder setup will not be discussed since it is simply half of the full system. That is, the full experimental setup is simply a duplication of the single pressure builder setup. The P&ID for the full experimental setup is shown in Figure 4.1 below.

The low-pressure side of each pressure multiplier has two tubes connected to it. All tubing is 0.25-inch copper tube for bendability and ease of modification. One tube connects to a ball valve that can be opened to vent the volume. The other tube is attached to a bottle of pressurized nitrogen at room temperature. The line has a pressure regulator that is used to fill the pressure multiplier volume with nitrogen at a set pressure. There is also a pressure transducer and thermocouple in line to measure the pressure and temperature of the volume.

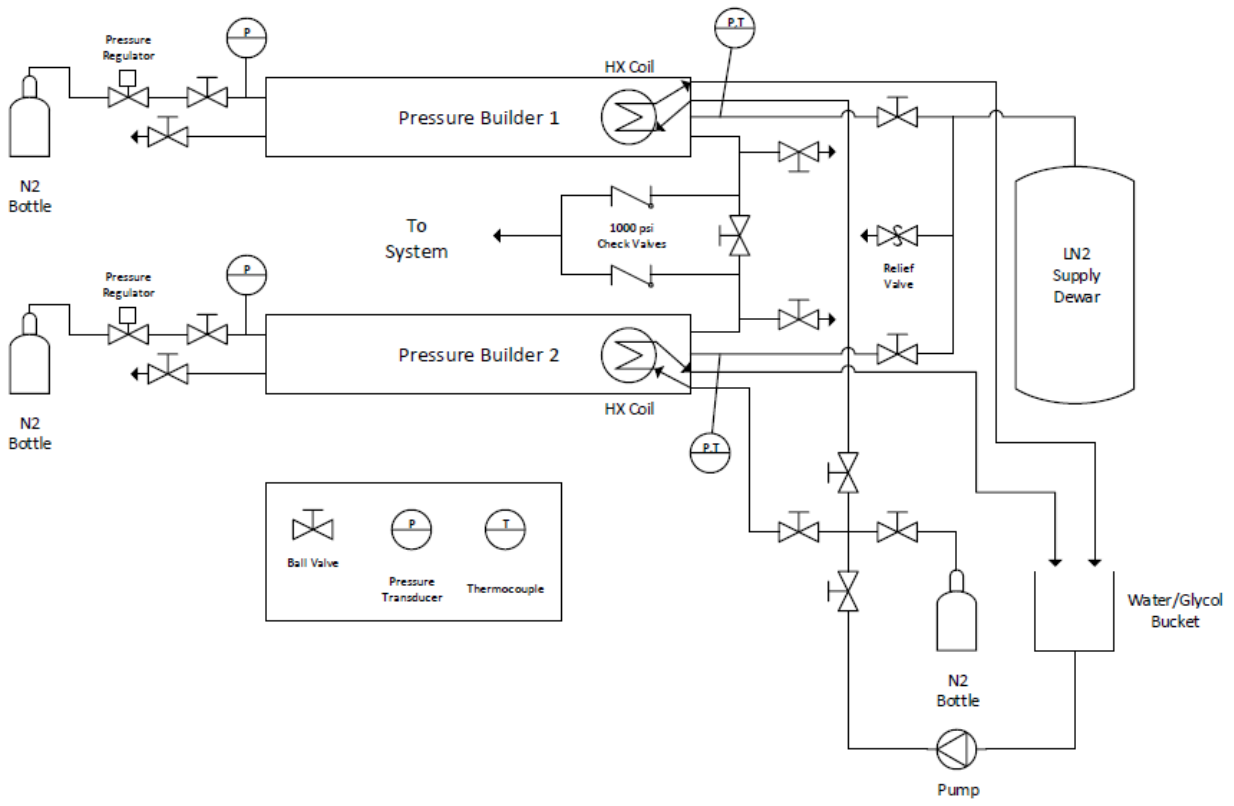

Figure 4.1. P&ID for the Two Pressure Builder Experimental Setup.

Each pressure builder high-pressure volume has four tubes connected: two for the nitrogen flow in and out of the volume and two for the internal heat exchanger coil inlet and outlet. The supply dewar has a single outlet for the liquid nitrogen flow. The line from the supply dewar splits into two lines that go into each pressure builder, separated and controlled by two ball valves. The dead volume between both valves has a safety relief valve to prevent over-pressurization. The inlets to each pressure builder have a thermocouple that is inserted directly into the volume. There is also a pressure transducer attached to the line to record the pressure inside the pressure builder volume. The pressure transducer is attached to the end of a pigtailed tube to prevent the coldest part of the flow from reaching the pressure transducer. All pressure

transducers also have snubbers attached to them to prevent damage from rapid changes in pressure.

The outlet lines from each pressure builder volume attached to each other via a ball valve, allowing the pressure builder-to-pressure builder venting process to occur. The outlets are also connected to each other through 1000 psi relief valves, whose outlets combine into a single line that connects to the ambient heat exchanger system. These relief valves allow the discharge process to occur when pressure builds up to 1000 psi. They also act as the safety relief for each pressure builder to prevent over-pressurization. For ease of experimentation, ball valves were also attached to the outlets to allow direct venting from each pressure builder at lower pressures.

After initial experimentation, it was determined that air was not a suitable fluid for the internal ambient heat exchangers. Thus, a glycol and water mixture was used to increase the rate of heat transfer. To implement this system, a bucket was filled with the glycol-water mixture. A line was connected to the bottom of the bucket and attached to a circulation pump that pumps the mixture through the internal coiled heat exchanger and back out into the bucket. The bucket was heated using heat tape to further increase the rate of heat transfer for the system. To prevent freezing of the glycol-water mixture when the heat exchanger wasn't running, a purging system had to be implemented. To achieve this, a pressurized air bottle was connected to the line that could be used to purge the tubes of liquid after the heat exchange was completed. A network of 4 ball valves was used to control flow of both the glycol-water mix and the air to both internal coiled heat exchangers. This system is not a practical method for heat exchange in the final system, but was used as an easier means of testing the rest of the proposed cycle.

4.2 TESTS AND PROCEDURES

Testing began initially with the pneumatically driven pressure builder. The pressure builder was first hydro-tested up to 3000 psi for safety and to test the welds. After passing the hydrostatic test, the first real test of the system was to see if it could build pressure up to the desired output of 1000 psi. The true intent of this test was to see if the system, as built, could build pressure to 1000 psi under "steady state" conditions. That is, after the entire system was cooled down, could enough liquid nitrogen be filled into the volume to achieve pressurization simply by heat addition? To cool down the system, liquid nitrogen was vented from the supply dewar through the entire pressure builder system. By expanding the cold nitrogen through the system, the rapid vaporization and flashing of the liquid cooled the system rapidly. After venting for about 10 to 15 minutes, the temperature inside the pressure builder dropped to about -170 ^{o}C, indicating that liquid was entering the pressure builder volume. After reaching this temperature, the pressure builder volume was closed off and the supply dewar was shut. Pressure rapidly rose in the pressure builder as the liquid nitrogen vaporized and expanded from the ambient heat addition. Through this testing, pressures in excess of 1000 psi were achieved and nitrogen flowed out of the system. The amount of mass and flowrate of discharged nitrogen were not measured since instrumentation capable of measuring the mass flow at such cold temperatures was not available. Another qualitative result of this test was the observation that blowing air through the internal coiled heat exchanger made no measurable difference on the rate of pressure building. This was most likely due to the relatively small surface area of the heat exchanger coil compared to the surface area of the entire pressure builder. Thus, it was decided to modify the internal heat exchanger system to use a glycol-water mixture to improve the heat transfer. However, after additional testing, the glycol-water mixture was not able to be pumped through the heat

exchanger coils without freezing. After testing solutions such as faster flow rates and preheating the glycol-water mixture up to 50 ^{o}C that still resulted in freezing, it was decided future designs should attempt to utilize a high surface area internal heat exchanger designed for air flow, instead of the coiled tube heat exchanger.

After verifying that the system could achieve the desired pressure building, a couple tests were conducted to validate some of the modeled processes. The first process tested was the pressure builder-to-pressure builder venting step. Since only one pressure builder was constructed at this time, a pressure vessel was used to simulate the volume of the second pressure builder. First, the pressure vessel was filled with nitrogen from the supply dewar, without first cooling off the volume. The pressure vessel was filled to a nominal pressure around 150 psi and a temperature around -30^{o}C. Next, the pressure builder volume was cooled down by venting liquid nitrogen from the supply dewar through the system. The pressure builder was closed off and pressure was allowed to build up to 1000 psi. Next, the pressures and temperatures of both the pressure vessel and the pressure builder were recorded and the valve connecting both volumes was opened immediately. As soon as a pressure equilibrium was reached, generally after about one second, pressures and temperatures were recorded for both volumes.

The experimental results were compared to the model, given the same initial conditions, as shown in Figure 4.2 and Figure 4.3 below. The data labeled “Bottle” refers to the pressure vessel acting as the second pressure builder volume. The initial results were not promising, showing errors in pressure and temperature up to 25%. Seeing that the temperature errors were all less than 10% for the bottle volume, it was hypothesized that the colder temperatures of the pressure builder were leading to model inconsistencies. The model utilized the measured initial pressure and temperature of each volume to determine the initial state, assuming an ideal gas at thermal

equilibrium. In reality, the cold gas had continuous heat addition from the surroundings, and the pressures and temperatures never steadied out. This means that the nitrogen mass that the model assumes may be very different from what was actually in each volume. Because the process model is driven by mass transfer, an error in the initial mass of each volume could lead to large discrepancies between the model and experimental results.

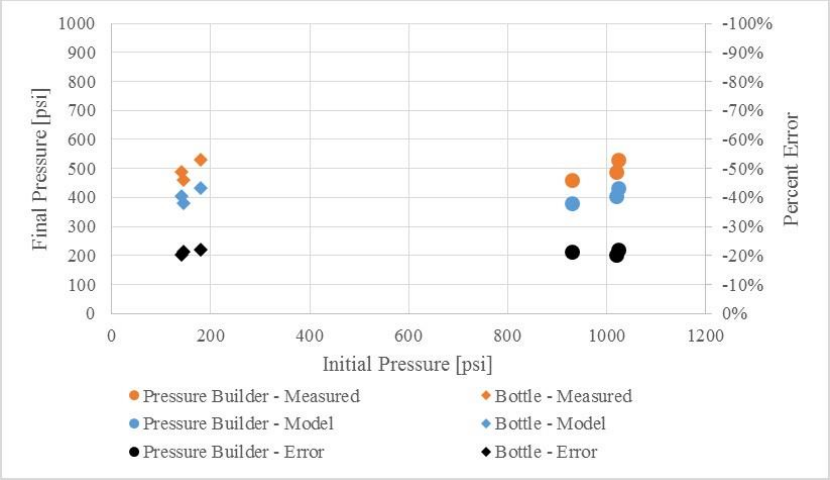

Figure 4.2. Experimental and Modeled Pressures for the Pressure Builder-to-Pressure Builder Venting Process Using Cold Nitrogen.

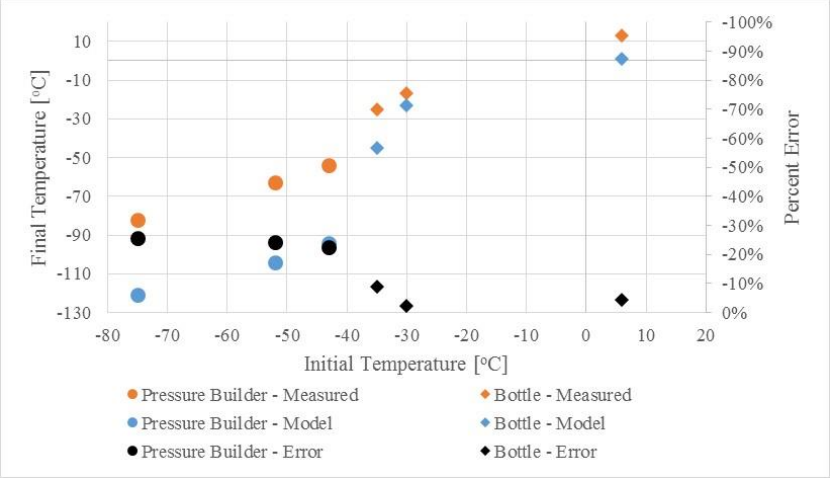

Figure 4.3. Experimental and Modeled Temperatures for the Pressure Builder-to-Pressure Builder Venting Process Using Cold Nitrogen.

To test this theory, the same test was repeated using room temperature nitrogen from high pressure bottles. The results of this second test are shown in Figure 4.4 and Figure 4.5 below.

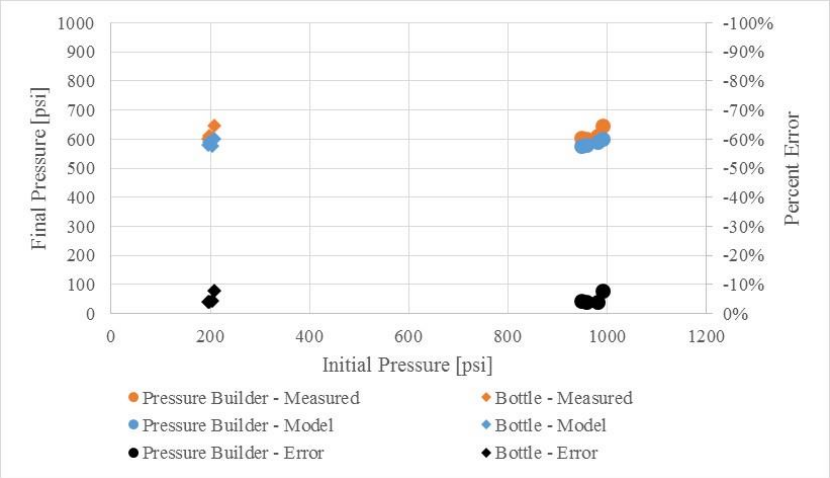

Figure 4.4. Experimental and Modeled Pressures for the Pressure Builder-to-Pressure Builder Venting Process Using Warm Nitrogen.

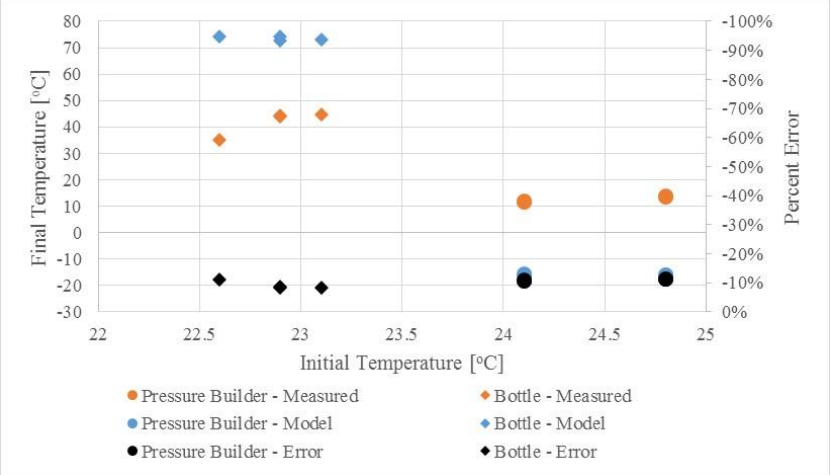

Figure 4.5. Experimental and Modeled Temperatures for the Pressure Builder-to-Pressure Builder Venting Process Using Warm Nitrogen.

The results of this test showed better overall agreement of both pressures and temperatures with the model. The pressure error was reduced to less than 5% is most cases and the temperature

error was reduced to about 10%. This shows that the model is more accurate for the process while closer to room temperature and the fundamentals of the process are being captured. With a lower temperature differential with ambient, the heat transfer into the volume is reduced and a more stable equilibrium is reached before and after the test to better establish the states for comparison with the model, leading to the more consistent results.

To further test the theory, the adiabatic expansion process was tested using cryogenic nitrogen. Adiabatic expansions are relatively simple and well understood processes so the experiment was expected to produce more agreeable results with the model. Figure 4.6 shows the results of this test.

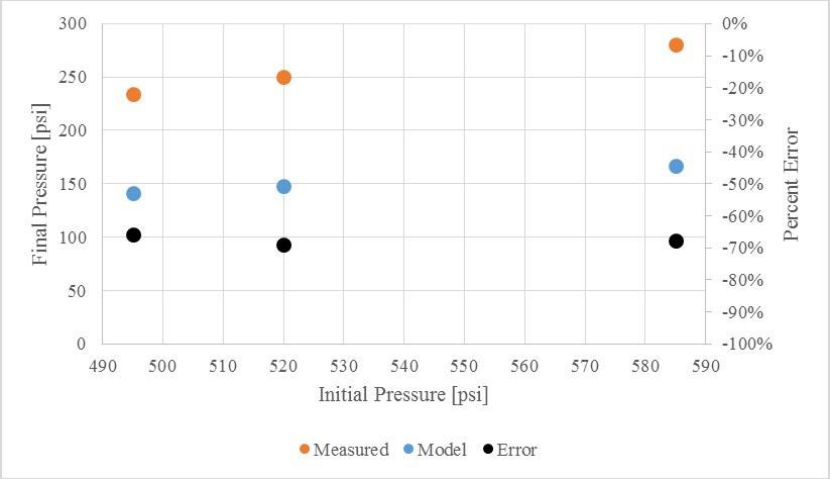

Figure 4.6. Experimental and Modeled Pressures for the Adiabatic Expansion Process.

As seen in Figure 4.6, the results did not agree with the model very well, approaching errors up to 70%. Once again, the error most likely arises from the unknown mass in the system and the constant ambient heat addition throughout the process due to the cold nitrogen temperature. It was determined that better agreement with the model may be obtained if the mass of the nitrogen in the pressure builder could be measured, providing a better description of the actual state in the

pressure builder. However, measuring the mass proved to be difficult due to the weight of nitrogen to be measured compared to the overall weight of the pressure builder. Due to cost and project time constraints, a mass measuring method was never developed. It was determined that exact agreement with the model was not as important as showing that the whole cycle could work as the model predicted. That is, could each step operate in succession and pressurize nitrogen to 1000 psi each cycle, regardless of precise agreement with the model predictions? In this way, similar to computational fluid dynamics, the model results could be used to influence design decisions and provide insight on the overall cycle while not necessarily providing precise physical results.

To this end, the final stage of testing began after construction of the second pressure builder system with the pressure multiplier was completed and integrated, as shown in the P&ID in Figure 4.1. Having already shown that the pressure builder could pressurize and discharge nitrogen at 1000 psi at the cold, steady-state conditions, the new test would operate the cycle from warm startup. The test starts by filling a pressure builder with nitrogen from the supply dewar. The nitrogen is then compressed while the second pressure builder is filled with nitrogen. Then, the first pressure builder vents into the second one and undergoes expansion. The first pressure builder is then refilled with nitrogen from the supply while the second pressure builder compresses. This process is repeated until the pressure after compression reaches the max pressure of 1000 psi and mass is discharged from the system. The point of this test is to ensure that the cycle can start up without wasting any nitrogen. Since the system starts at room temperature, the nitrogen flashes very quickly, requiring a large number of cycles to occur rapidly to ensure cool down of the system. If the system can reach 1000 psi and discharge, while

still being able to drop pressure below the supply dewar through the venting and expansion steps, the cycle would be proven viable.

As testing began for this setup, it was discovered that the piston seals in both pressure builders could no longer maintain their seal. The leaks by the pistons were too significant to conduct any valid testing with the two pressure builder system. While the exact reason for the seal failure could not be determined, it is likely the seals in the first pressure builder design failed after the first few tests but went unnoticed due to the other side of the piston being pressurized. Due to the failure of the OmniSeal O-ring design for this application, a new sealing method must be designed and implemented in order to validate the cycle. A promising seal design that was not fully explored in this study is the Bridgman seal [11]. This seal utilizes the pressure of the system to engage the seal, preventing leaks at high pressures. While the Bridgman seal was not initially developed for cryogenic use, the design could be modified to adapt to cryogenic temperatures. Once a working cryogenic piston seal is developed, the cycle can be tested in full.

Chapter 5. CONCLUSIONS AND FUTURE WORK

5.1 CONCLUSIONS

The first major result of this study is the conclusion that cryogenic refrigeration is not a feasible process to integrate into the vaporization and pressure building device. As found through the modeling and results discussed in Sections 2.3 and 2.4, and shown in Figure 2.3 and Figure 2.4, cryogenic refrigeration requires changing volumes in order to be a viable process. This is due to the inability to complete the heat addition process of the refrigeration cycle before a temperature equilibrium between the refrigerant and the nitrogen in the pressure builder is reached. Once changing volumes are considered, it no longer makes sense to utilize refrigeration as a means for pressure reduction when a simple volume expansion can achieve the same results with less work input, design complexity, and cost.

Moreover, the seven step cycle with changing volumes, discussed in Section 2.6 and Section 2.7, provides the theoretical foundation for a working cycle that can achieve the desired nitrogen pressurization with no venting. This cycle effectively uses volume expansions and pressure builder-to-pressure builder venting processes to achieve the needed pressure reduction without venting any nitrogen product. Initial tests proved the cycle, and the mechanical design presented in Chapter 3, could achieve pressurization to 1000 psi. Additional testing for complete cycle validation is ongoing.

5.2 FUTURE WORK

The piston seals are one of the most significant design challenges that must still be overcome. The development of reliable, dynamic cryogenic seals is of critical importance to the success of the proposed thermodynamic cycle. A potential sealing method that was not fully

pursued is a modified version of a Bridgman seal. By adapting the Bridgman seal design for use in a cryogenic system, suitable piston sealing for the pressure builder may be achieved. This seal design could also see future use in a wide variety of cryogenic applications due to the current unavailability of high pressure, dynamic cryogenic seals.

A better method of ambient heat addition could be considered as an alternative to the coiled tube heat exchanger used in the designs tested here. As discussed in Section 4.2, the coiled tube internal heat exchanger was ineffective with both air and the glycol-water mixture as working fluids. Sticking with air as the working fluid for the ambient heat addition would be ideal for design and operational simplicity. Thus, a high surface area compact heat exchanger would be a design worth considering to achieve the desired heat addition.

After conducting numerous tests with prototype devices in lab, it is proposed that downsizing the whole system could be advantageous for the rapid development and testing of prototypes and may even be required for operation of a final, full scale design. The relatively large mass and thermal inertia of the current prototypes add to the startup time of the cycle by increasing the amount of nitrogen that is needed to cool off the system to achieve steady state operation. Reducing the size of the device may improve startup times and overall efficiency by reducing flashing losses for the nitrogen. In addition, a smaller diameter pressure builder volume may enable the use of a linear actuator to drive the compression process, by reducing the force required for compression. This may even enable a motor and camshaft design that could drive multiple pressure builders in parallel. This new device would work similar to a traditional combustion engine in a car, except in reverse. A smaller system would also allow for the use of a more accurate scale that could measure the mass of nitrogen in the system, providing more useful information on the performance of the system as well as a better means of validation for

the model. One complication of working with a smaller pressure builder is that the ambient heat addition will make up a larger proportion of the energy transfer in the system, making all the adiabatic assumptions made in the model harder to enforce in practice. To mitigate this problem, a more significant effort will need to be made to insulate the pressure builder from the environment, perhaps even submerging the whole pressure builder in a vat of liquid nitrogen.

In addition to decreasing the size of the pressure builder, it is recommended to replace all the manual ball valves with solenoid or air actuated valves. Experiments conducted with the current setup were relatively slow due to the time it takes to switch multiple valves. This created problems due to the constant ambient heat addition from the surroundings that contributed to the difficulties with the model validation effort discussed in Section 4.2. By replacing the manual valves with controllable valves, the entire cycle can be automated to maximize the speed at which it operates, mitigating the heat addition problem while operating the pressure builder as it would in its final implementation.

In conclusion, working cryogenic piston seals must first be developed in order to fully validate the proposed thermodynamic cycle. Once working seals are developed, the full cycle can be validated and the overall design can be iterated upon, taking into consideration the suggestions made above.

BIBLIOGRAPHY

[1] "Nitrogen (N2) Properties, Uses and Applications Nitrogen Gas and Liquid Nitrogen," Universal Industrial Gases, Inc...Nitrogen N2 Properties, Uses, Applications - Gas and Liquid Available: http://www.uigi.com/nitrogen.html.

[2] Knowlen, C., Williams, J., Mattick, A. T., Deparis, H., and Hertzberg, A., "Quasi-Isothermal Expansion Engines for Liquid Nitrogen Automotive Propulsion," SAE Technical Paper Series, Jun. 1997.

[3] Knowlen, C., Mattick, A. T., Bruckner, A. P., and Hertzberg, A., "High Efficiency Energy Conversion Systems for Liquid Nitrogen Automobiles," SAE Technical Paper Series, Nov. 1998.

[4] Knowlen, C., Mattick, A. T., Bruckner, A. P., and Hertzberg, A., "High Efficiency Energy Conversion Systems for Liquid Nitrogen Automobiles," SAE Technical Paper Series, Nov. 1998.

[5] Williams, J., Knowlen, C., Mattick, A., and Hertzberg, A., "Frost-Free Cryogenic Heat Exchangers for Automotive Propulsion," 33rd Joint Propulsion Conference and Exhibit, Jun. 1997.

[6] Kimura, R., "Numerical and Experimental Study of an Ambient Air Vaporizer Coupled with a Compact Heat Exchanger," thesis, 2017.

[7] Çengel, Y. A., and Boles, M. A., Thermodynamics: An Engineering Approach, New York, NY: McGraw-Hill, 2011.

[8] Lemmon, E.W., Huber, M.L., McLinden, M.O. NIST Standard Reference Database 23: Reference Fluid Thermodynamic and Transport Properties-REFPROP, Version 9.1, National Institute of Standards and Technology, Standard Reference Data Program, Gaithersburg, 2013.

[9] Budynas, R. G., and Nisbett, J. K., "Stresses in Pressurized Cylinders," Shigley's Mechanical Engineering Design, New York, NY: McGraw-Hill, 2011, pp. 113–114.

[10] Saint-Gobain. OmniSeal Spring-Energized Seals Product Handbook. Saint-Gobain Performance Plastics, 2014. Available: http://www.seals.saint-gobain.com/sites/imdf.seals.com/files/saint-gobainseals_omniseal_handbook_na.pdf.

[11] Bridgman, P. W., "The Technique of High Pressure Experimenting," Proceedings of the American Academy of Arts and Sciences, vol. 49, 1914, pp. 627–643.

APPENDIX A

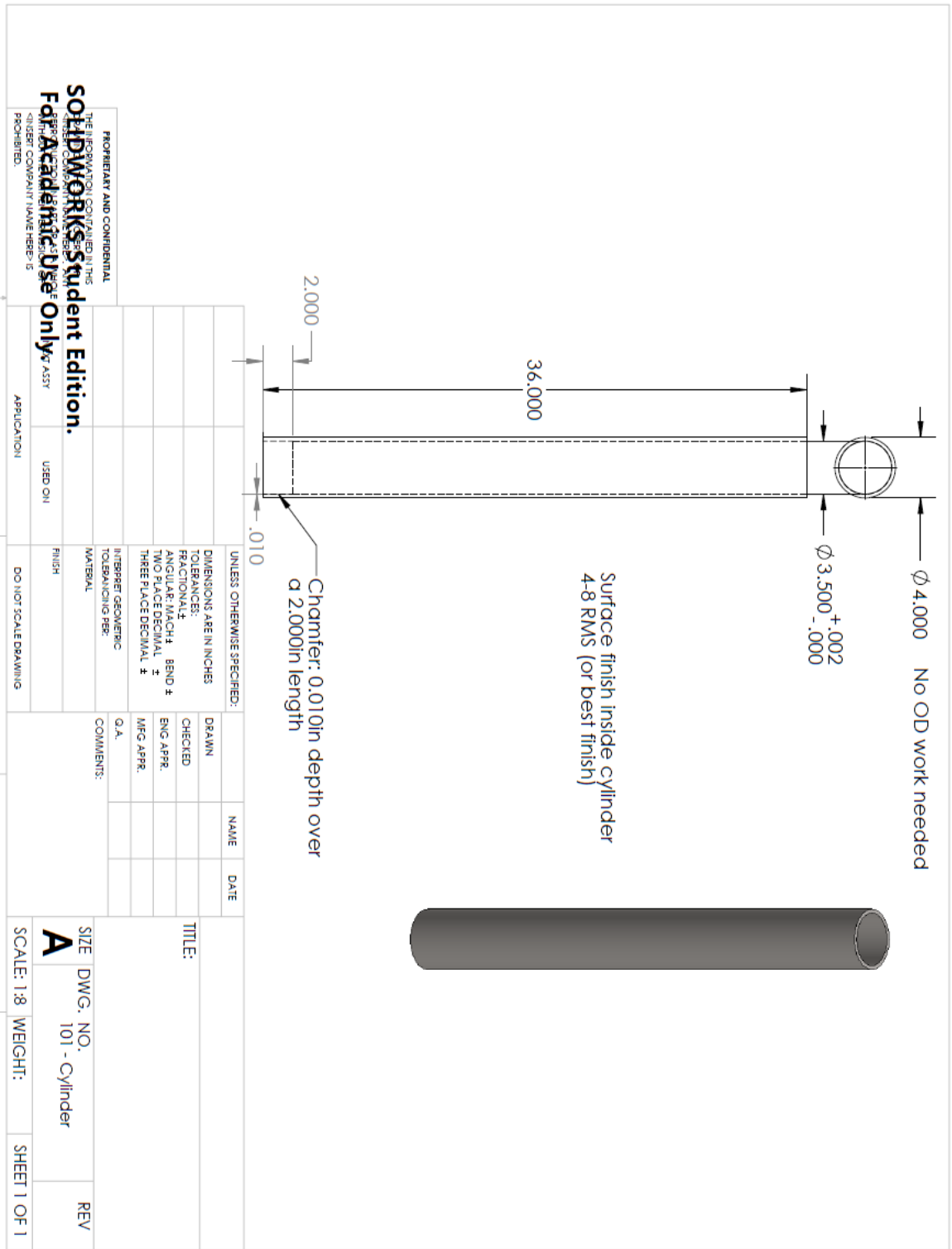
Ø4.000 No OD work needed
Ø3.500 +.002 -.000
Surface finish inside cylinder
4-8 RMS (or best finish)
36.000
2.000
.010
Chamfer: 0.010in depth over
a 2.000in length
PROPRIETARY AND CONFIDENTIAL
SOLIDWORKS Student Edition.
For Academic Use Only.
UNLESS OTHERWISE SPECIFIED:
DIMENSIONS ARE IN INCHES
TOLERANCES:
FRACTIONAL ±
ANGULAR: MACH ± BEND ±
TWO PLACE DECIMAL ±
THREE PLACE DECIMAL ±
INTERPRET GEOMETRIC
TOLERANCING PER:
MATERIAL
FINISH
NEXT ASSY
USED ON
APPLICATION
DO NOT SCALE DRAWING
DRAWN
CHECKED
ENG APPR.
MFG APPR.
Q.A.
COMMENTS:
NAME
DATE
TITLE:
SIZE
A
DWG. NO.
101 - Cylinder
REV
SCALE: 1:8
WEIGHT:
SHEET 1 OF 1

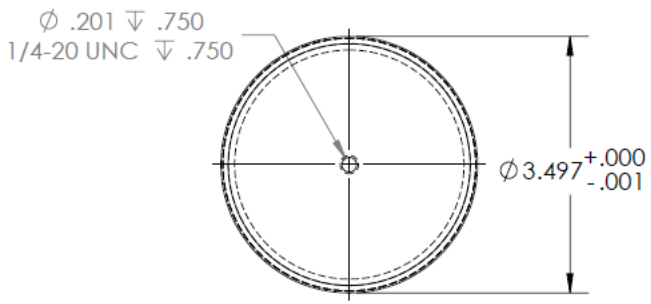

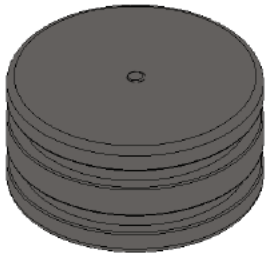

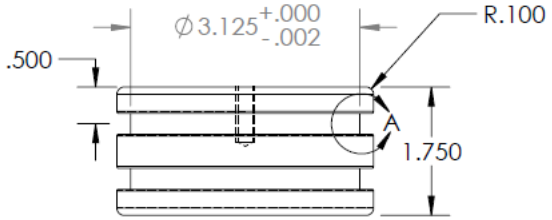

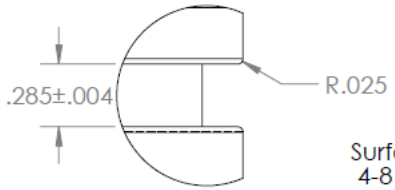

DETAIL A
SCALE 1.5 : 1

Surface finish in Grooves
4-8 RMS (or best finish)

Surface finish on Piston Sides
4-8 RMS (or best finish)

		UNLESS OTHERWISE SPECIFIED:		NAME	DATE
		DIMENSIONS ARE IN INCHES TOLERANCES: FRACTIONAL ± ANGULAR: MACH ± BEND ± TWO PLACE DECIMAL ± THREE PLACE DECIMAL ±	DRAWN		
			CHECKED		
			ENG APPR.		
			MFG APPR.		
		INTERPRET GEOMETRIC TOLERANCING PER:	Q.A.		
		MATERIAL 304 Stainless Steel	COMMENTS:		
		FINISH			
NEXT ASSY	USED ON				
APPLICATION		DO NOT SCALE DRAWING			

TITLE:

SIZE	DWG. NO.	REV
A	102 - Piston	
SCALE: 1:2	WEIGHT:	SHEET 1 OF 1

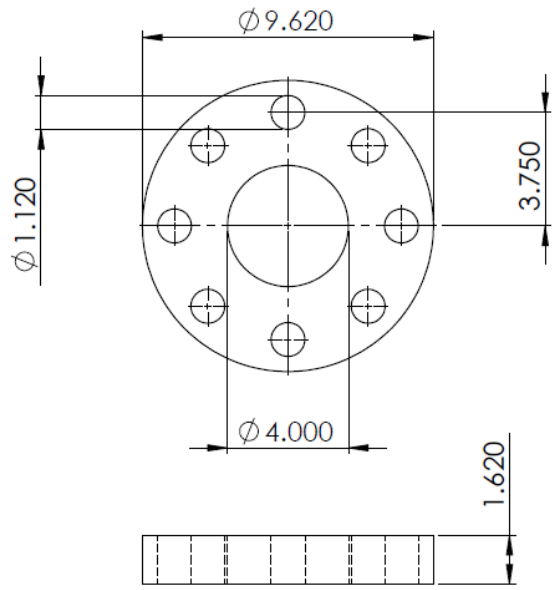

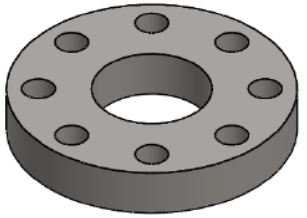

		UNLESS OTHERWISE SPECIFIED:		NAME	DATE
		DIMENSIONS ARE IN INCHES TOLERANCES: FRACTIONAL ± ANGULAR: MACH ± BEND ± TWO PLACE DECIMAL ± THREE PLACE DECIMAL ±	DRAWN		
			CHECKED		
			ENG APPR.		
			MFG APPR.		
		INTERPRET GEOMETRIC TOLERANCING PER:	Q.A.		
		MATERIAL	COMMENTS:		
NEXT ASSY	USED ON	FINISH			
APPLICATION		DO NOT SCALE DRAWING			

TITLE:

SIZE	DWG. NO.	REV
A	001 - Bored Flange	
SCALE: 1:5	WEIGHT:	SHEET 1 OF 1

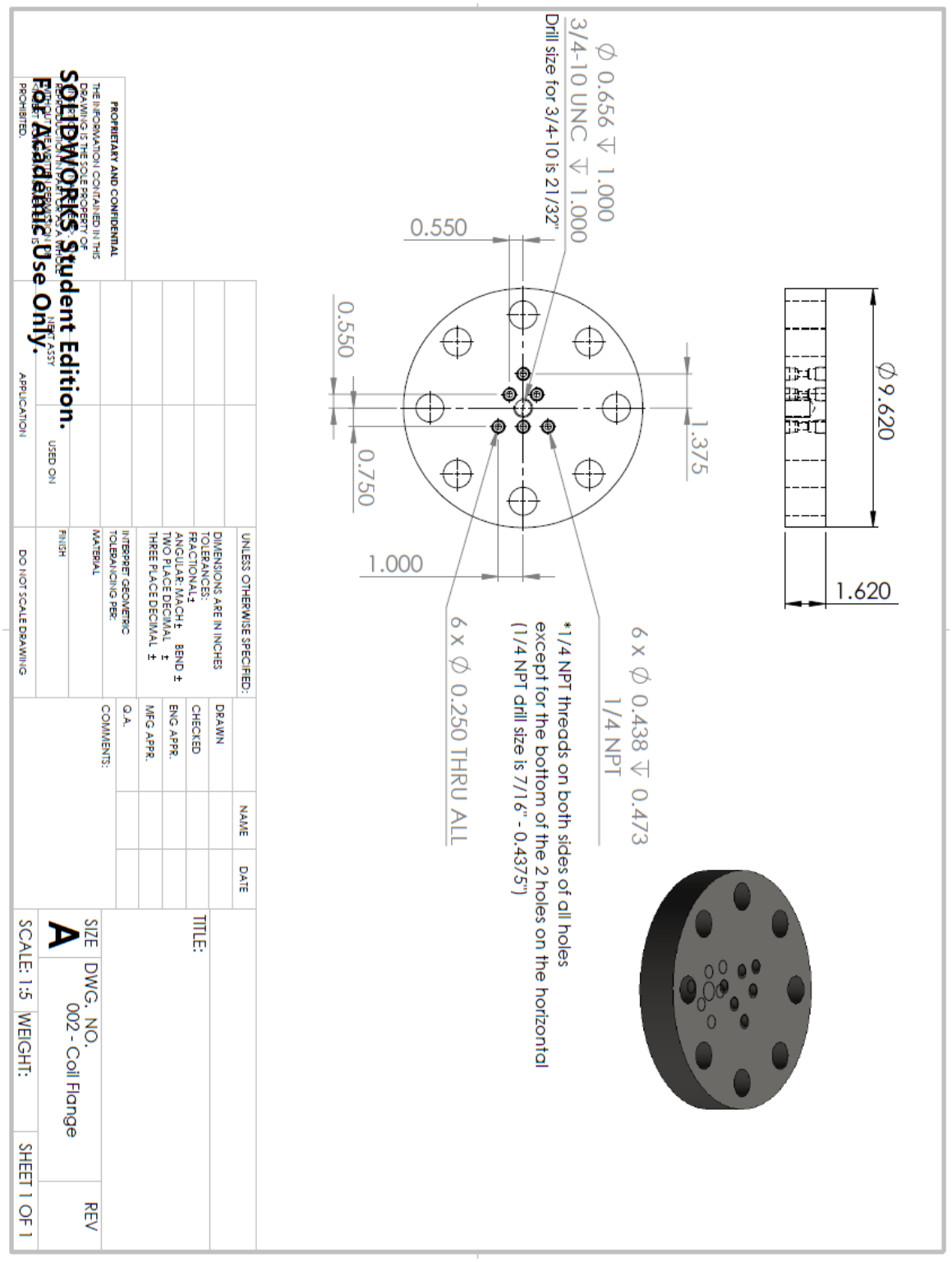
Ø 9.620
1.620
Ø 0.656 ∓ 1.000
3/4-10 UNC ∓ 1.000
Drill size for 3/4-10 is 21/32"
0.550
0.550
1.375
0.750
1.000
6 x Ø 0.438 ∓ 0.473
1/4 NPT
6 x Ø 0.250 THRU ALL
*1/4 NPT threads on both sides of all holes
except for the bottom of the 2 holes on the horizontal
(1/4 NPT drill size is 7/16" - 0.4375")
PROPRIETARY AND CONFIDENTIAL
THE INFORMATION CONTAINED IN THIS
DRAWING IS THE SOLE PROPERTY OF
UNLESS OTHERWISE SPECIFIED:
DIMENSIONS ARE IN INCHES
TOLERANCES:
FRACTIONAL ±
ANGULAR: MACH ± BEND ±
TWO PLACE DECIMAL ±
THREE PLACE DECIMAL ±
INTERPRET GEOMETRIC
TOLERANCING PER:
MATERIAL
FINISH
DO NOT SCALE DRAWING
DRAWN
CHECKED
ENG APPR.
MFG APPR.
Q.A.
COMMENTS:
NAME
DATE
USED ON
NEXT ASSY
APPLICATION
TITLE:
SIZE
A
DWG. NO.
002 - Coil Flange
REV
SCALE: 1:5
WEIGHT:
SHEET 1 OF 1
SOLIDWORKS Student Edition.
For Academic Use Only.

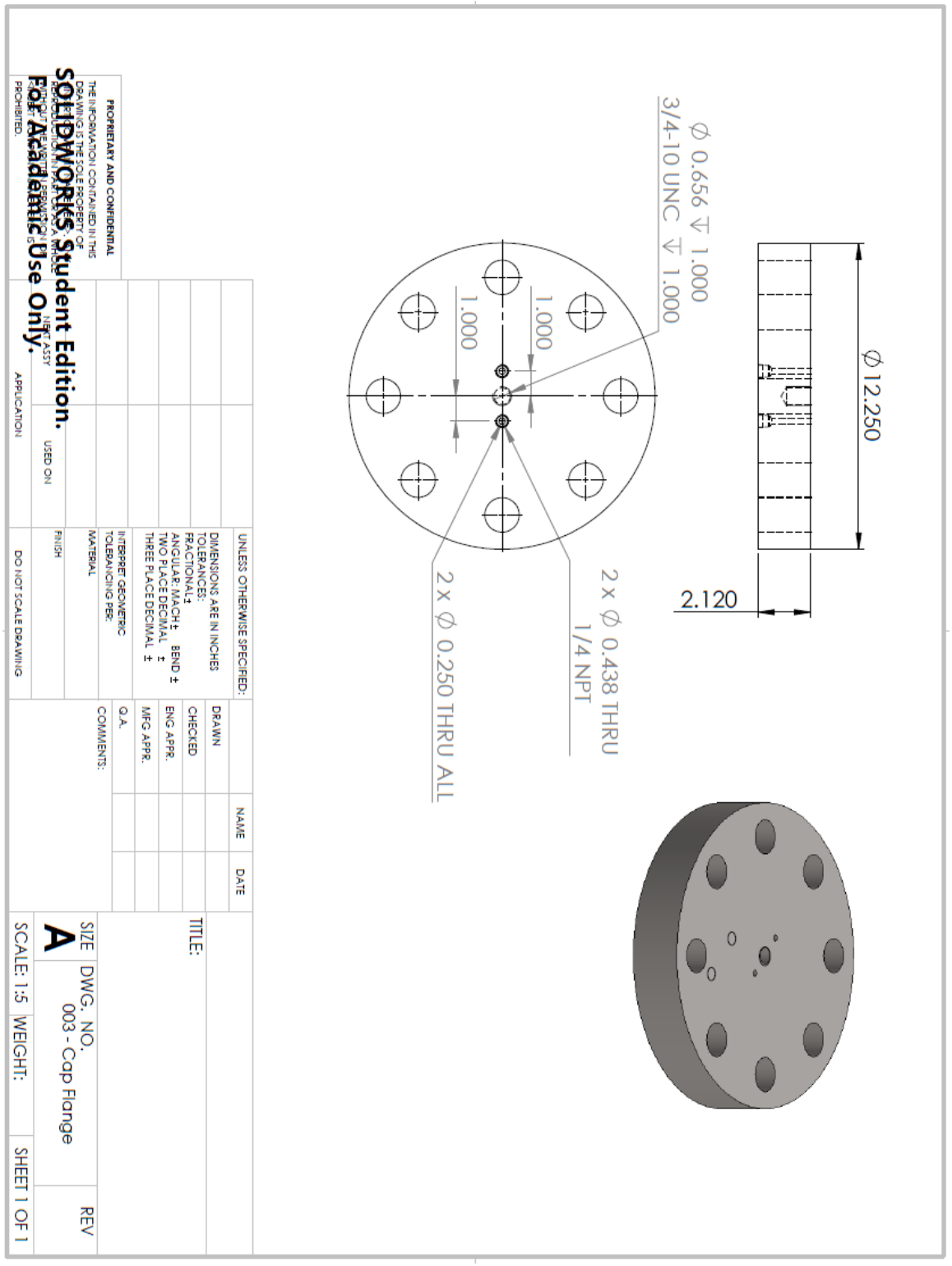
⌀ 12.250
2.120
⌀ 0.656 ↧ 1.000
3/4-10 UNC ↧ 1.000
1.000
1.000
2 x ⌀ 0.438 THRU
1/4 NPT
2 x ⌀ 0.250 THRU ALL
UNLESS OTHERWISE SPECIFIED:
DIMENSIONS ARE IN INCHES
TOLERANCES:
FRACTIONAL ±
ANGULAR: MACH ± BEND ±
TWO PLACE DECIMAL ±
THREE PLACE DECIMAL ±
INTERPRET GEOMETRIC
TOLERANCING PER:
MATERIAL
FINISH
NEXT ASSY
USED ON
APPLICATION
DO NOT SCALE DRAWING
NAME
DATE
DRAWN
CHECKED
ENG APPR.
MFG APPR.
Q.A.
COMMENTS:
TITLE:
SIZE
A
DWG. NO.
003 - Cap Flange
REV
SCALE: 1:5
WEIGHT:
SHEET 1 OF 1
PROPRIETARY AND CONFIDENTIAL
THE INFORMATION CONTAINED IN THIS
DRAWING IS THE SOLE PROPERTY OF
PROHIBITED.
SOLIDWORKS Student Edition.
For Academic Use Only.

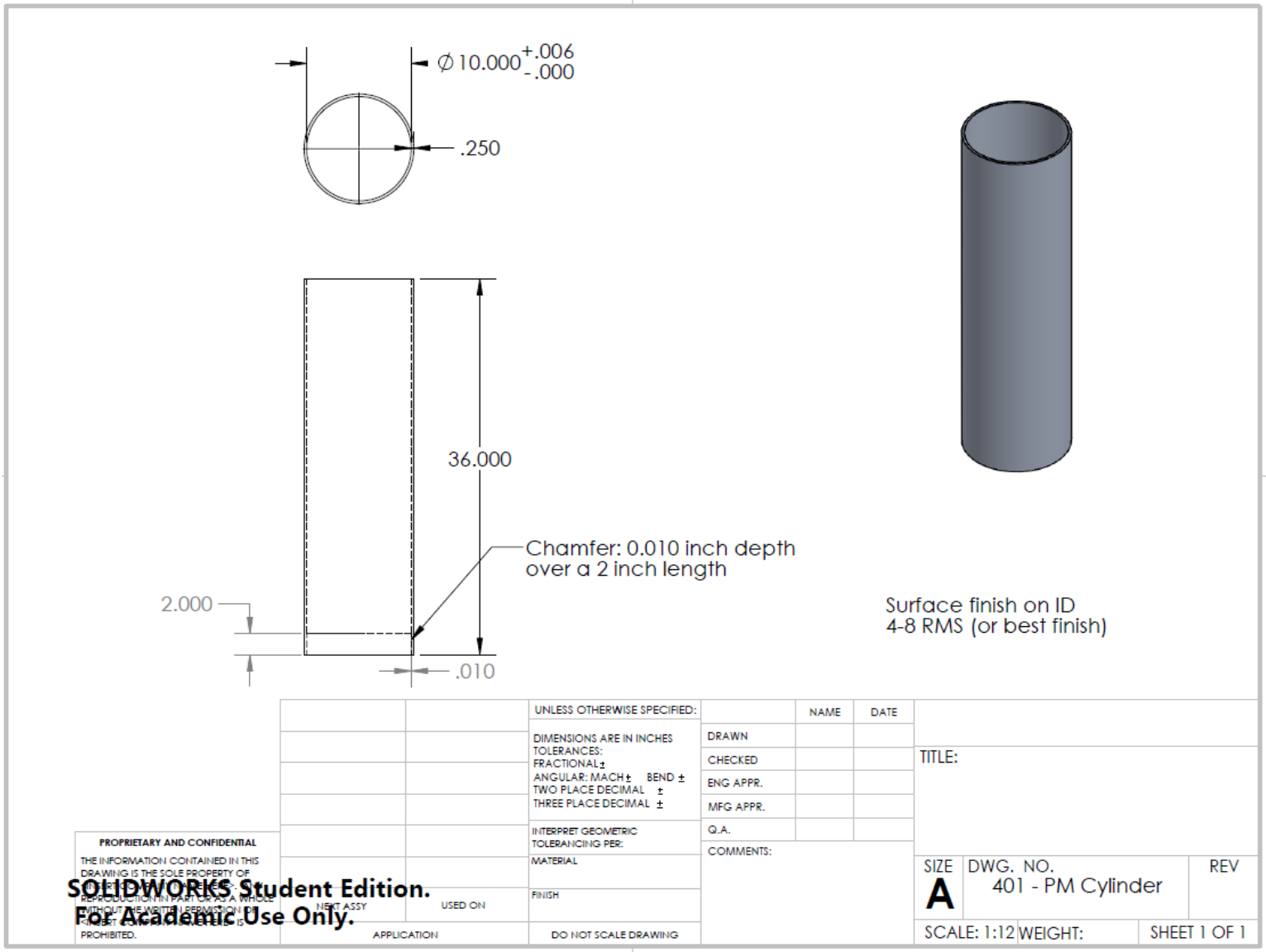

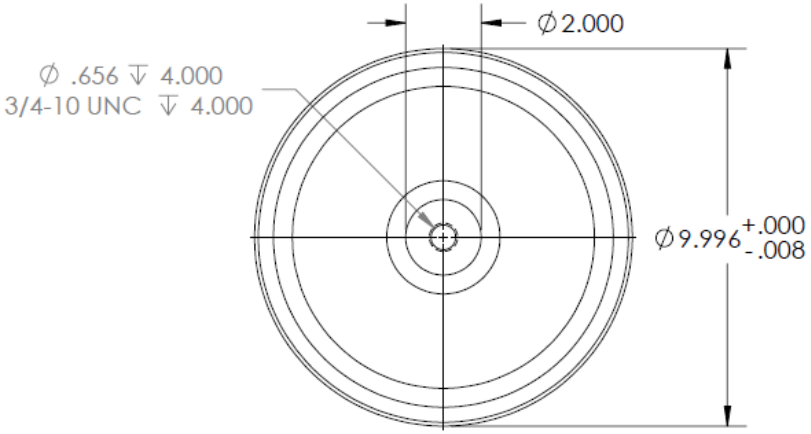

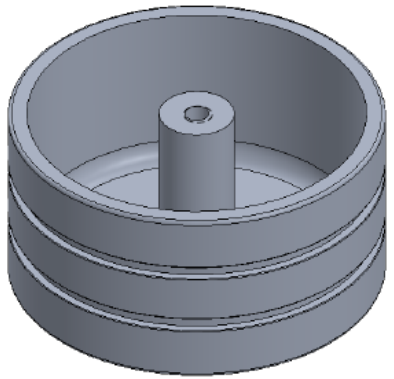

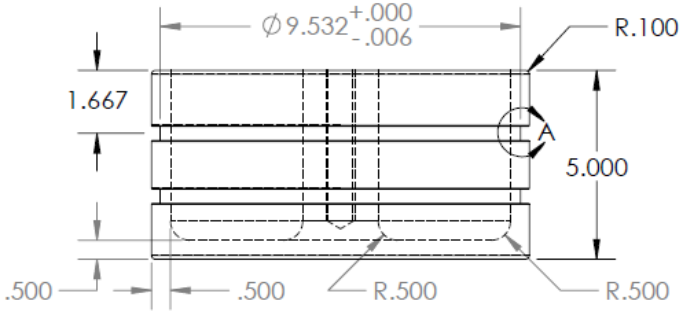

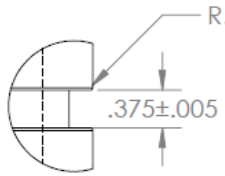

DETAIL A
SCALE 1 : 1.5

Surface Finish in Grooves
32 RMS

Surface Finish on Piston Sides
4-8 RMS (or best finish)

		UNLESS OTHERWISE SPECIFIED:		NAME	DATE
		DIMENSIONS ARE IN INCHES TOLERANCES: FRACTIONAL ± ANGULAR: MACH ± BEND ± TWO PLACE DECIMAL ± THREE PLACE DECIMAL ±	DRAWN		
			CHECKED		
			ENG APPR.		
			MFG APPR.		
		INTERPRET GEOMETRIC TOLERANCING PER:	Q.A.		
		MATERIAL Aluminum 6061-T6511	COMMENTS:		
NEXT ASSY	USED ON	FINISH			
APPLICATION		DO NOT SCALE DRAWING			

TITLE:

SIZE	DWG. NO.	REV
A	402 - PM Piston	
SCALE: 1:4	WEIGHT:	SHEET 1 OF 1

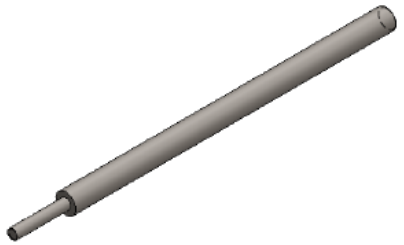

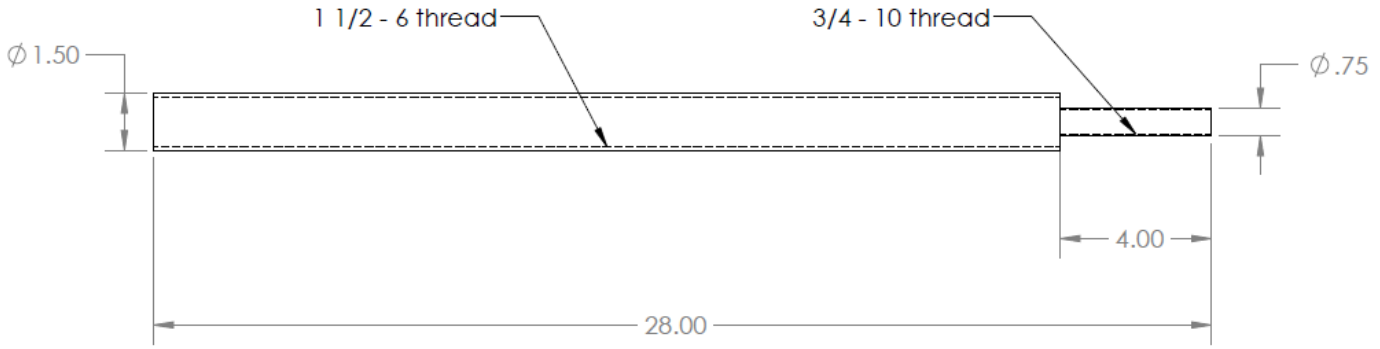

		UNLESS OTHERWISE SPECIFIED:		NAME	DATE
		DIMENSIONS ARE IN INCHES TOLERANCES: FRACTIONAL ± ANGULAR: MACH ± BEND ± TWO PLACE DECIMAL ± THREE PLACE DECIMAL ±	DRAWN		
			CHECKED		
			ENG APPR.		
			MFG APPR.		
		INTERPRET GEOMETRIC TOLERANCING PER:	Q.A.		
		MATERIAL	COMMENTS:		
NEXT ASSY	USED ON	FINISH			
APPLICATION		DO NOT SCALE DRAWING			

TITLE:

SIZE	DWG. NO.	REV
A	805 - Tie Rod - All Thread	
SCALE: 1:8	WEIGHT:	SHEET 1 OF 1

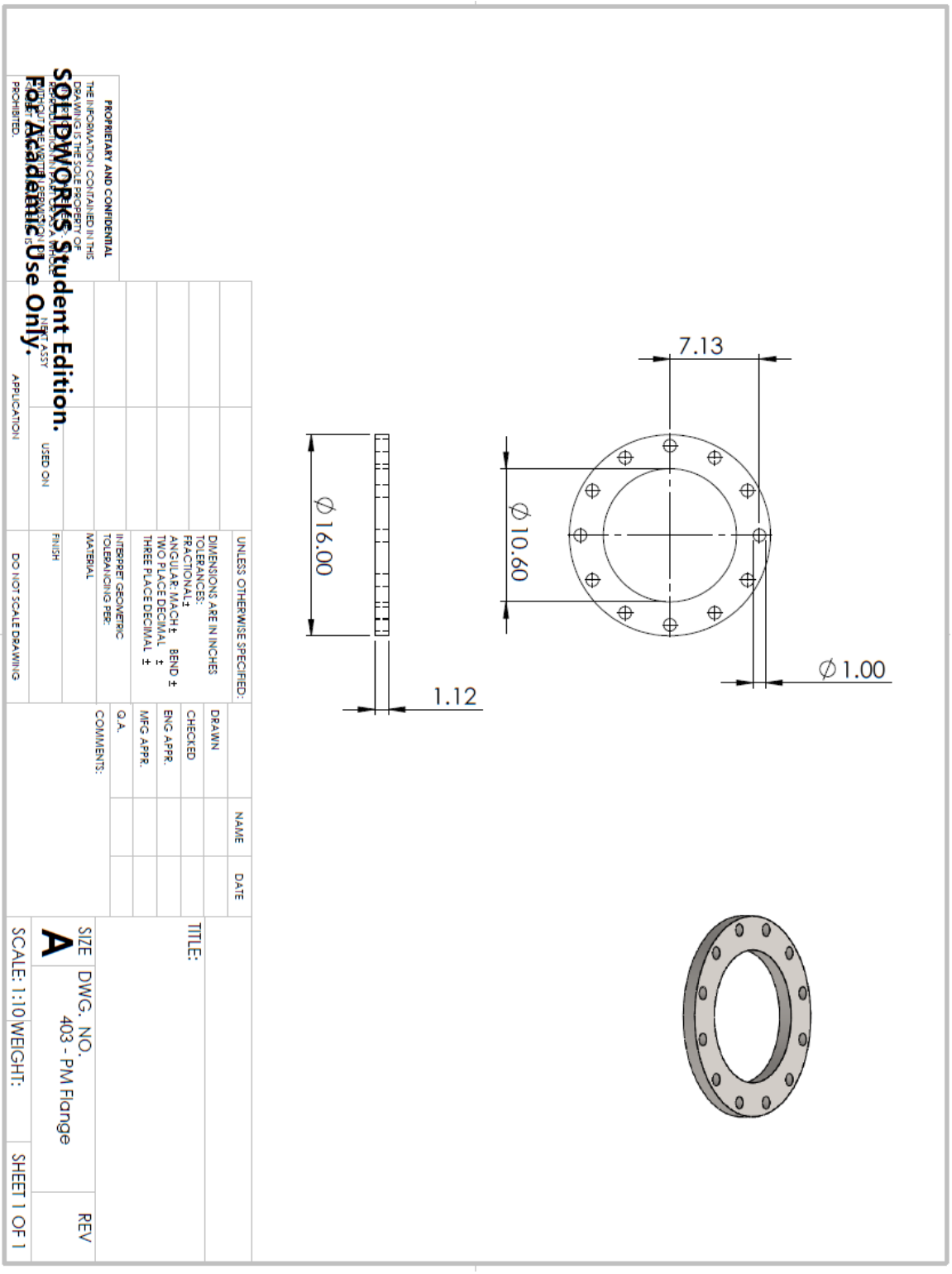
7.13
∅ 10.60
∅ 1.00
∅ 16.00
1.12
UNLESS OTHERWISE SPECIFIED:
DIMENSIONS ARE IN INCHES
TOLERANCES:
FRACTIONAL ±
ANGULAR: MACH ± BEND ±
TWO PLACE DECIMAL ±
THREE PLACE DECIMAL ±
INTERPRET GEOMETRIC
TOLERANCING PER:
MATERIAL
FINISH
DO NOT SCALE DRAWING
NAME
DATE
DRAWN
CHECKED
ENG APPR.
MFG APPR.
Q.A.
COMMENTS:
TITLE:
SIZE
A
DWG. NO.
403 - PM Flange
REV
SCALE: 1:10 WEIGHT:
SHEET 1 OF 1
NEXT ASSY
USED ON
APPLICATION
PROPRIETARY AND CONFIDENTIAL
THE INFORMATION CONTAINED IN THIS
DRAWING IS THE SOLE PROPERTY OF
REPRODUCTION IN PART OR AS A WHOLE
WITHOUT THE WRITTEN PERMISSION OF
PROHIBITED.
SOLIDWORKS Student Edition.
For Academic Use Only.

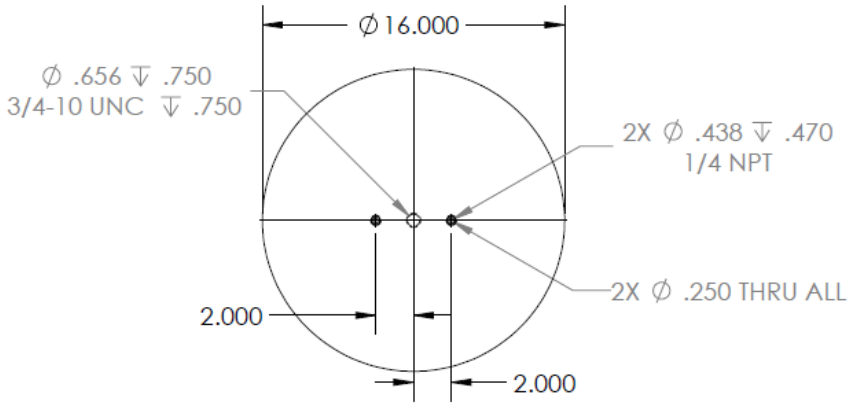

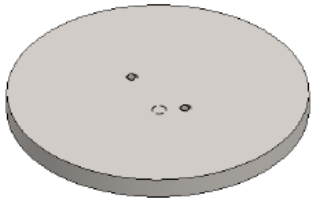

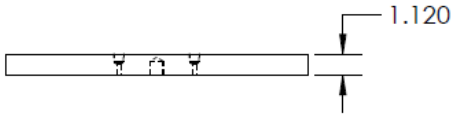

UNLESS OTHERWISE SPECIFIED:		NAME	DATE		
DIMENSIONS ARE IN INCHES TOLERANCES: FRACTIONAL ± ANGULAR: MACH ± BEND ± TWO PLACE DECIMAL ± THREE PLACE DECIMAL ±	DRAWN			TITLE:	
	CHECKED				
	ENG APPR.				
	MFG APPR.				
INTERPRET GEOMETRIC TOLERANCING PER:	Q.A.				
MATERIAL	COMMENTS:			SIZE A	DWG. NO. 404 - PM Flange Cap
FINISH					REV
NEXT ASSY / USED ON				SCALE: 1:8	WEIGHT: / SHEET 1 OF 1
APPLICATION / DO NOT SCALE DRAWING					

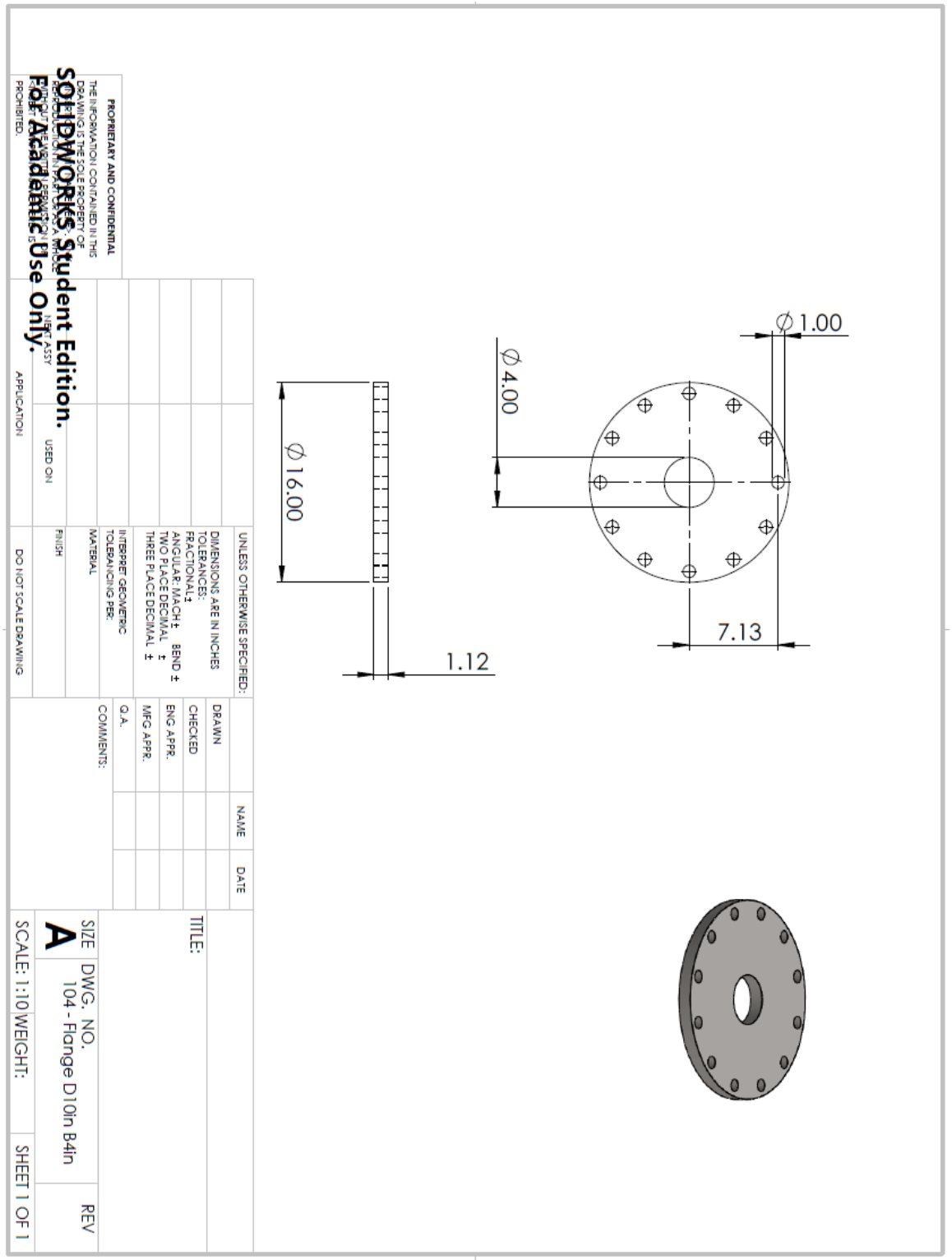
∅1.00
∅4.00
7.13
∅16.00
1.12
PROPRIETARY AND CONFIDENTIAL
THE INFORMATION CONTAINED IN THIS
DRAWING IS THE SOLE PROPERTY OF
SOLIDWORKS Student Edition.
For Academic Use Only.
NEXT ASSY
USED ON
APPLICATION
DO NOT SCALE DRAWING
UNLESS OTHERWISE SPECIFIED:
DIMENSIONS ARE IN INCHES
TOLERANCES:
FRACTIONAL ±
ANGULAR: MACH ± BEND ±
TWO PLACE DECIMAL ±
THREE PLACE DECIMAL ±
INTERPRET GEOMETRIC
TOLERANCING PER:
MATERIAL
FINISH
NAME
DATE
DRAWN
CHECKED
ENG APPR.
MFG APPR.
Q.A.
COMMENTS:
TITLE:
SIZE
A
DWG. NO.
104 - Flange D10in B4in
REV
SCALE: 1:10 WEIGHT:
SHEET 1 OF 1